



Article

Life Cycle Assessment of Post-Combustion CO₂ Capture and Recovery by Hydrophobic Polypropylene Cross-Flow Hollow Fiber Membrane Contactors with Activated Methyldiethanolamine

Aytac Perihan Akan ^{1,2,3,*} , John Chau ¹, Gulen Gullu ²  and Kamalesh K. Sirkar ¹

¹ Center for Membrane Technologies, Otto H. York Department of Chemical and Materials Engineering, New Jersey Institute of Technology, Newark, NJ 07102, USA

² Department of Environmental Engineering, Hacettepe University, 06800 Ankara, Turkey

³ Graduate School of Science and Engineering, Hacettepe University, 06800 Ankara, Turkey

* Correspondence: apakan@hacettepe.edu.tr

Abstract: The present study evaluated the environmental impacts of post-combustion CO₂ capture and recovery via membrane–gas absorption processes. We have used SimaPro v.9 packages with the Ecoinvent v3.5 database employing two different methods, ReCiPe 2016 Endpoint (H) and Midpoint (H), considering a fundamental methodological framework to determine the most environmentally friendly experimental condition. Life cycle impact categories were examined and assessed supposing a functional unit of 1 kgCO₂/h recovered. Fourteen environmental impact categories including global warming, ozone depletion, eutrophication, and toxicity potentials have been evaluated within the context of a gate-to-gate approach focusing on only the process stage. Simulation results showed that the maximum liquid flow rate, sweep helium flow rate together with the minimum solvent concentration demonstrated the highest impact on human health, ecosystem, and resources. The usage of pure methyldiethanolamine (MDEA) activated by piperazine as a reactive absorbent provided the lowest environmental impact due to the elimination of the energy needed to heat and evaporate water present in aqueous absorbent solutions and the prevention of the excess water consumption depending on meeting the water needed for reactive absorption of CO₂ in tertiary amine MDEA from simulated humidified flue gas stream. The study highlights the importance of LCA in the determination of an environmentally more sustainable condition during the capture and recovery of post-combustion CO₂ by gas absorption and stripping using membrane contactors in tertiary amine MDEA.

Keywords: post-combustion CO₂ capture; life cycle assessment; membrane contactor; environmental impact; absorption; stripping



Citation: Akan, A.P.; Chau, J.; Gullu, G.; Sirkar, K.K. Life Cycle Assessment of Post-Combustion CO₂ Capture and Recovery by Hydrophobic Polypropylene Cross-Flow Hollow Fiber Membrane Contactors with Activated Methyldiethanolamine. *Atmosphere* **2023**, *14*, 490. <https://doi.org/10.3390/atmos14030490>

Academic Editor: Kumar Vikrant

Received: 23 January 2023

Revised: 22 February 2023

Accepted: 27 February 2023

Published: 1 March 2023



Copyright: © 2023 by the authors. Licensee MDPI, Basel, Switzerland. This article is an open access article distributed under the terms and conditions of the Creative Commons Attribution (CC BY) license (<https://creativecommons.org/licenses/by/4.0/>).

1. Introduction

There is no doubt that one of the vital threats facing the world in the last decades is global warming, based on the increase in the concentration of greenhouse gases, including carbon dioxide (CO₂), methane (CH₄), and nitrous oxide (N₂O) caused particularly by human activities, which will substantially and inevitably impact future generations [1–3]. It is a well-known fact that CO₂, which considerably comes from the burning of carbon-based fossil fuels, such as coal, petroleum, and natural gas in order to generate electricity for meeting 68% of the world's energy needed for especially a variety of industries, such as iron and steel, cement, chemicals, and petroleum releasing remarkable emissions into the atmosphere, is the largest contributor to the enhanced greenhouse effect bringing about global warming and other environmental issues [4–10]. CO₂ concentrations in the atmosphere have exhibited a remarkable increase from pre-industrial times (approximately

280 ppm) to recently (418.90 ppm) as of July 2022 [10,11]. According to the International Energy Agency (IEA) report in 2018, global CO₂ emissions depending on fuel combustion were 32.31 GtCO₂ in 2016 and reached 33.1 GtCO₂ in 2018 [3,12]. Although global CO₂ emissions decreased by 5.8% in 2020 due to the COVID-19 pandemic, the demand for carbon-based energy has caused global energy-related CO₂ emissions to remain at the level of 31.5 Gt, which means that the average CO₂ concentration of 412.5 ppm in the atmosphere for 2020 is about 50% more than that during the industrial revolution [13]. It is expected that approximately 50% of electricity generation will come from fossil fuels by 2040, and in parallel, combustion-based electricity generation will continue to be a major source of CO₂ emissions released into the atmosphere [3].

To reduce the influence of energy-based environmental problems, which are among the most significant issues of the 21st century and directly affect most countries' economies and people's lives, some effective approaches, such as improving energy efficiency, promoting energy conservation, increasing the use of low-carbon fuels, developing renewable energies, adopting geoengineering approaches such as afforestation and reforestation, and investigating carbon capture and storage (CCS) technologies, are being taken into account by decision-makers [6,8,14]. Among them, CCS which consists of the processes of capture, transport, and long-term storage of CO₂, and has been used since 1920 for commercial purposes, is a promising method to separate CO₂ from a gas mixture in the flue gas emitted from power plant emissions to mitigate CO₂ emissions in the atmosphere. This method requires high CO₂ storage capacity [8,15–17]. CCS technologies are commonly divided into three groups: pre-combustion, post-combustion, and oxy-fuel combustion [8,18]. Post-combustion CO₂ capture stands out among other technologies and is more widely preferred, as it can be easily integrated into the existing facilities of many different industries such as power plants, the chemical industry, and the fuel, iron and steel, and cement industries [8,19]. In post-combustion CO₂ capture, amine scrubbing, adsorption, cryogenic distillation, and membrane processes are the most preferred techniques [2,7,20,21]. Among these technologies, the most mature amine-based CO₂ capture absorption process results in the highest removal efficiency to separate CO₂ from flue gas in conventional gas-liquid contactors, but it requires high energy demand and increases environmental concerns based on the use and generation of toxic materials during the solvent production used in the chemical absorption [7,22]. Hence, alternative CO₂ capture strategies consisting of absorption using novel solvents, such as ionic liquid, calcium looping, adsorption based on materials, such as zeolites, metal-organic frameworks, carbon nanotubes, and activated carbons, and membrane technologies are being studied to replace the conventional technology based on absorption with amines [17,23].

Membrane-based CO₂ capture technologies, first applied in the early 1990s for the separation of CO₂ from flue gas, have gained much more attention because of their superior properties, such as operational simplicity, high reliability, low environmental impact, and eco-friendliness [21,24]. In this regard, membrane processes can be an alternative solution to absorption technology when considering environmental aspects [25]. Since CCS technologies, which are preferred for the reduction of anthropogenic CO₂ emissions, may cause effects on the ecosystem and human health due to the consumption of resources in the form of more energy and materials and the formation of chemical by-products, it is recommended to apply life cycle assessment (LCA), which represents a powerful tool to evaluate the most significant environmental impacts of CO₂ capture technologies to assess and compare the real sustainability of the CO₂ capture processes regarding all environmental aspects [3,5,26–28].

LCA is a standardized methodology and the most common technique that enables a comprehensive assessment of the environmental impacts of a certain product or process by using the “cradle to grave” approach over the whole system lifetime [26,29–32]. LCA evaluates depletion of the resource and formation of emissions during the whole life cycle of a product or a process from thousands of human activities, such as the extraction of raw materials, transport, production, and packaging overuse of the product to reuse, recycle,

and final disposal of wastes, each of which needs to be documented to determine environmentally significant material and energy flows [33–35]. Therefore, LCA can be considered a beneficial guide to evaluating emissions based on CO₂ capture technologies [28].

Up to now, many studies have focused on multiple environmental impacts stemming from post-combustion CO₂ capture technologies [1,32,36–46]. It should be particularly highlighted that the majority of the present works investigating the LCA modeling approach to evaluate the environmental impacts of post-combustion CO₂ capture based on different methodologies have focused on pilot-scale research, such as natural gas combined cycle power plants [47–49]. It is of great importance to determine the environmental effects of studies that deal with CO₂ capture efficiency for different operating conditions at the lab scale, depending on chemical absorption, adsorption, or membrane processes that support sustainable development goals (SDG) in the fight against climate change, which will guide the pilot scale studies. In a study published by Olabi and co-workers (2023) [50], it was stated that membrane-based carbon capture technologies have a positive effect on SDG13, which is related to combating climate change, by reducing CO₂ emissions in coal-fired thermal power plants by up to 90%. For this reason, in addition to only a few recent studies assessing the environmental impacts of membrane–gas separation and membrane contactors known as membrane-based carbon capture processes by addressing the pilot-scale studies available so far in the literature [21,28,30], LCA analyses related to membrane-based CO₂ capture depending on the experimental studies are also currently needed. Compared to previous studies, the present study first investigates the LCA of post-combustion CO₂ capture and recovery on a lab scale, in which pure activated methyldiethanolamine (aMDEA) in crossflow membrane contactors with coated hollow fibers were used. Thus, it will be the first to shed light on the LCA of post-combustion CO₂ capture and recovery by evaluating the environmental impact of a membrane–gas absorption process employing tertiary amine MDEA as a reactive absorbent considering the experimental results.

2. Materials and Methods

2.1. Materials

Microporous hydrophobic polypropylene hollow fibers were used in membrane contactors for both cross-flow absorption and stripping modules developed by Applied Membrane Technology (Minnetonka, MN, USA). Detailed information about the dimensions and properties of the hollow fiber membrane modules is presented in [51]. The absorbent liquid used was aMDEA obtained by adding ~1% piperazine (PZ) from Sigma Aldrich (Milwaukee, WI, USA) to MDEA from Fisher Scientific (Hanover Park, IL, USA). To obtain aqueous solutions, deionized water was used. The preparation procedure for aqueous absorbents in three different compositions performed in the present study namely, (i) 80 vol% aMDEA/20 vol% water, (ii) 90 vol% aMDEA/10 vol% water, and finally (iii) pure aMDEA, is explained in a previous research publication [51]. In absorption and stripping experiments, a feed gas, which represents a simulated flue gas mixture consisting of 14.1% CO₂, 1.98% O₂, and balance N₂ (Airgas, Oakland, NJ, USA), was humidified using a porous hydrophobic polypropylene hollow-fiber-based humidification module to mimic real flue gas in a power plant and to activate the reaction between MDEA and CO₂ in the case of pure MDEA being used as the absorbent [51].

2.2. Experimental Set-Up and Procedure

A simulated feed gas mixture was fed from the gas cylinder into the humidification module before entering the absorption module where it was passed through the lumen side of the hollow fibers in the absorption module. The feed gas flow rate was controlled via a multi-channel mass flow controller (model 8248A, Matheson TRI-GAS, Montgomeryville, PA, USA) and mass flow controller transducer (model 8272-0452, Matheson TRI-GAS, Montgomeryville, PA, USA). Experiments were conducted with feed gas flow rates in the range of 50–300 cm³/min. Liquid flow rates controlled by the liquid flow meter ((1-GPI

Model GM001S2C41-20.317 cm (1/8") NPT s. steel oval gear meter, Great Plains Industries, Wichita, KS, USA) were 15.10, 16.60, and 18.90 L/h for all experiments.

The experiment started with the circulation of the absorbent liquid from a liquid reservoir to hollow fiber membrane contactors to fill up the contactors with the absorbent liquid. Then, the absorbent liquid was introduced by a micro-pump (pump head model GJ-N21-JF1SJ, pump motor model DG-F61.G1T2P5.J.B., Micropump, Vancouver, WA, USA) through a flow meter and passed through the shell side of hollow fibers in the absorption module by a tubular loop immersed in water to reach a temperature of around 50–55 °C. The CO₂-loaded absorbent liquid was fed into the heat exchanger to raise its temperature from 50–55 °C to 85–90 °C. Then, the absorbent at the exit of the heat exchanger was fed into the shell side of the stripper. This absorbent liquid was passed through a tubular loop immersed in an oil bath heated up to 95–110 °C. The heated and stripped liquid was returned to the heat exchanger to cool down. In the present study, to obtain the CO₂ concentration at the stripper outlet, the liquid returned from the heat exchanger was not discharged into the reservoir; it was pumped directly into the absorption module to prevent the introduction of the rich-solvent into the reservoir. A schematic representation describing the experimental set-up used in the present study is exhibited in Figure 1. Unlike the alternatives in the previous studies [52,53], in the system introduced in Figure 1, feed gas was passed through the bore side of hollow fibers and the absorbent was introduced in cross flow into the shell side of fibers in hollow fiber membrane contactors since polymeric hollow fibers offer 5–10 times bigger interfacial area than conventional gas absorption methods when feed gas is introduced into the bore of hollow fibers for a short period [54,55].

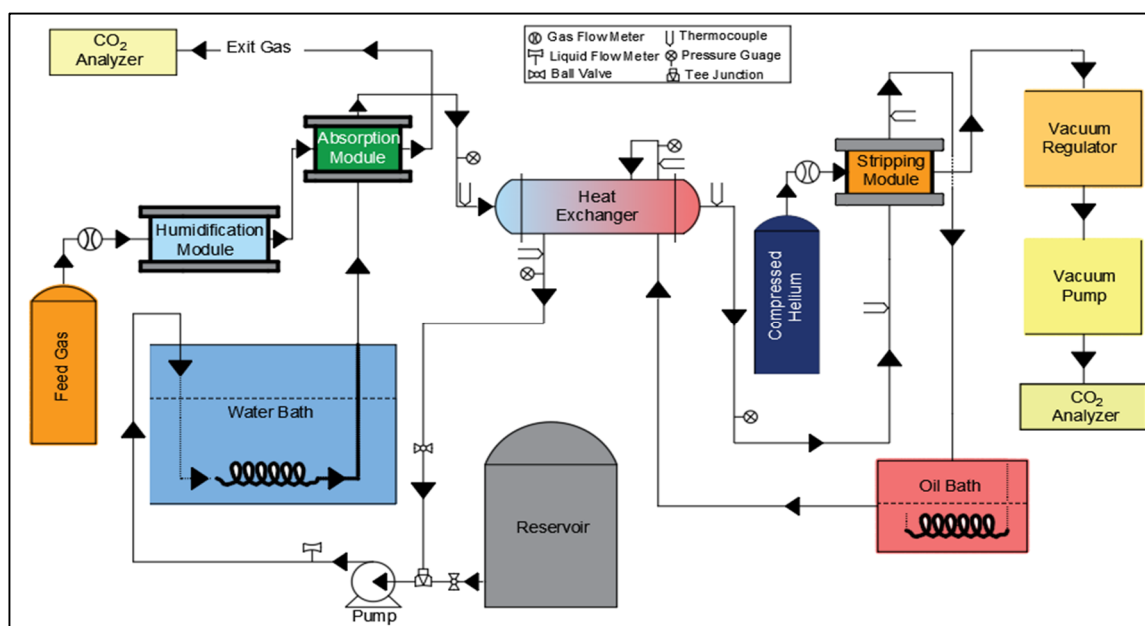


Figure 1. Schematic diagram of the experimental setup with bypassing reservoir and both sweep helium and vacuum for stripping mode. Reprinted with permission from references [51]; This article was published in Separation and Purification Technology, 244, 116427, Akan, A.P.; Chau, J.; Sirkar, K.K., Post-combustion CO₂ capture and recovery by pure activated methyldiethanolamine in crossflow membrane contactors having coated hollow fibers, Copyright Elsevier (2020), [54], This article was published in Journal of Membrane Science, 471, Mulukutla, T.; Obuskovic, G.; & Sirkar, K. K., Novel scrubbing system for post-combustion CO₂ capture and recovery: Experimental studies, 16–26, Copyright Elsevier (2014). Copyright Elsevier (2020, 2014).

To measure CO₂ concentration at the exit of the tube side on the absorber, a solid-state IR-based CO₂ analyzer (model 906, Quantek, Grafton, MA, USA) with a low resolution was used. On the stripper side, helium gas was passed through the bore of the stripping

module to remove and collect the stripped CO₂ from the CO₂-loaded absorbent; the exiting gas containing stripped CO₂ in helium was subjected to a controlled vacuum by a vacuum pump, and a vacuum regulator by referring an alternative method for the stripping process [54]. Its CO₂ concentration was measured by another Quantek CO₂ analyzer [51].

Additional information on experimental procedures and equipment in the experimental setup and also schematic representations of both the absorbent flow around the fiber outside and the rectangular box arrangement are available in [51,54].

3. Life Cycle Assessment Methodology

The present study was intended to provide an assessment of the environmental impact based on post-combustion CO₂ capture and recovery via membrane–gas absorption processes using SimaPro v.9 packages with the Ecoinvent v3.5 database. Two different methods, ReCiPe 2016 Endpoint (H) and Midpoint (H), were used considering a fundamental methodological framework, which was established by the International Standards Organization (ISO) and comprises four phases: (i) definition of goal and scope, (ii) inventory analysis, (iii) impact assessment, and finally interpretation [56,57].

3.1. Goal and Scope

The goal and scope phase comprises the definition of the aim of the LCA study, the system boundary, and the functional unit [27]. Here the intended use of the LCA is defined, system boundaries are set, and the functional unit is selected [26]. The goal and scope of the study are to determine the environmental impacts of different operating conditions, including feed gas flow rate, liquid flow rate, and absorbent concentration values, based on post-combustion CO₂ capture and recovery via the synergistic effects of chemical absorption and membrane permeation through the polypropylene membrane coated with fluorosiloxane in a membrane contactor and aMDEA hybrid systems. As the focus of the study is on the CO₂ capture and recovery processes, the scope of the study is from the “gate to gate” approach.

3.1.1. Functional Unit

A functional unit can measure the performance of a system [58]. For the environmental comparison of very different technological systems, a fixed reference point, or in other words, a consistent functional unit, is a basis for comparison [30,58]. This study assumed to recover 1 kg CO₂ within 1 h to evaluate the results globally; all assumptions were implemented by a functional unit of 1 kgCO₂/h recovered.

3.1.2. System Boundary

In the LCA approach, system boundaries are intended from cradle to grave to comprise all burdens and impacts in the life cycle of a product or a process, so that the inputs into the system become major resources [59]. In the present study, a gate to gate approach is considered because it only evaluates the processing approach in absorption and stripping modules to capture and recover the CO₂ emissions from a simulated feed gas stream without other stages of the LCA approach, such as manufacturing, transportation, and disposal of wastes. The overall system boundary of post-combustion CO₂ capture and recovery by pure aMDEA in crossflow membrane contactors having coated hollow fibers for both absorption and stripping processes is exhibited in Figure 2.

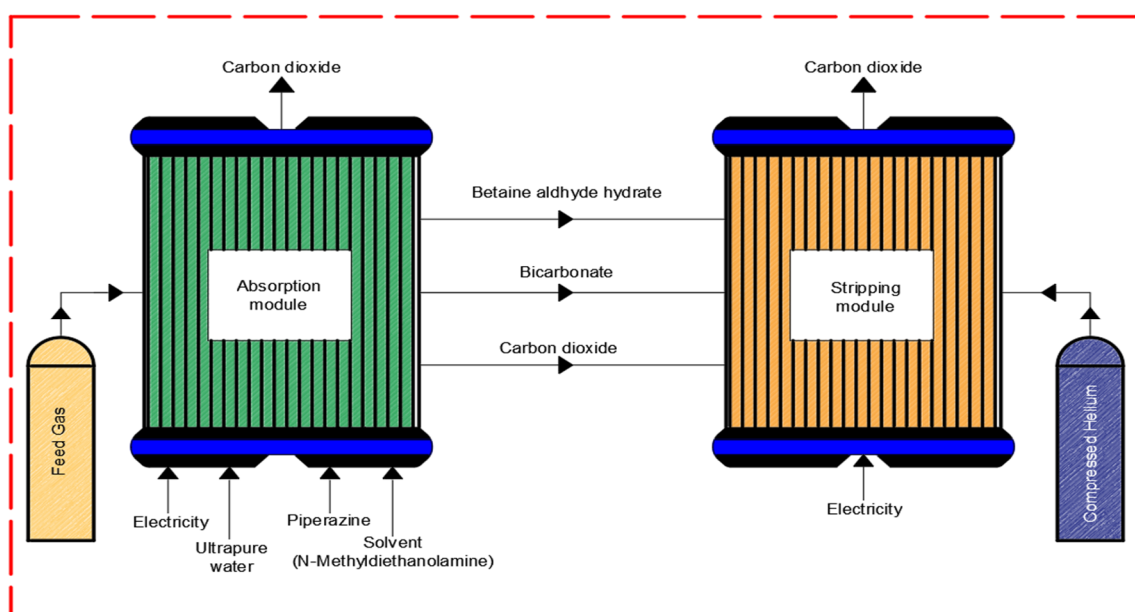


Figure 2. The overall system boundary of post-combustion CO₂ capture and recovery by cross-flow hollow fiber membrane contactors for both absorption and stripping processes.

Post-combustion CO₂ capture and recovery by pure aMDEA in crossflow membrane contactors having coated hollow fibers is composed of two fundamental stages: the first step occurs in the absorption module in which humidified simulated feed gas is passed through the bores of the hollow fiber membrane absorber module and the absorbent liquid, passing into a water bath to reach around 40–45 °C. The feed gas is also pumped into the absorber module in cross-flow for CO₂ absorption. After that, the CO₂-loaded absorbent is sent to a heat exchanger where the absorbent is heated to 85–90 °C.

In the second stage, the heated CO₂-loaded absorbent is then pumped to the shell side of the membrane stripping module. The stripped absorbent solution is cooled somewhat; it is then sent to an oil bath for heating and then is sent to the heat exchanger where it heats the CO₂-loaded absorbent exiting the membrane absorber. After substantially cooling the spent absorbent in the heat exchanger, it is directly sent to the membrane absorber module for CO₂ absorption. To measure exit CO₂ concentration on the strip side, helium gas was passed through the bore of the stripping module; the exiting gas containing stripped CO₂ in helium was subjected to a controlled vacuum by a vacuum pump and a vacuum regulator [51].

3.2. Life Cycle Inventory

The LCA data for post-combustion CO₂ capture and recovery provided by membrane contactors in the absorption and stripping processes are taken from the commercially available Ecoinvent v3.5 database from SimaPro v.9 software. The life cycle impacts depending on materials and energy were obtained from a series of energy and mass balances based on each set of experimental data. The primary inputs to the absorber module include a simulated flue gas mixture, consisting of 14.1% CO₂, 1.98% O₂, and balance N₂, solvents, including N-methyldiethanolamine and piperazine, energy, and pure water, whereas CO₂ emissions released into the atmosphere and CO₂ in the absorbent solution can be considered as outputs for the absorber membrane contactor. In the stripping process, energy, compressed helium gas, and CO₂ in the absorbent solution coming from the outlet of the absorber module are accepted as inputs, whereas stripped CO₂ can be considered as the sole output from the module. The inventory data for 1 kg/h recovered is provided in Table S1 in the Supplementary Materials, and has been obtained from mass balances between inputs and outputs for both absorption and stripping membrane contactors.

In the inventory phase of the LCA, some assumptions listed below had been applied to implement LCA studies:

The present study was carried out in New Jersey, USA; hence, the inputs needed to enter into the SimaPro software like electricity were selected from the data inventory characteristic of the USA for analyzing the environmental impacts of the study. In other words, electricity was denoted as “medium voltage US market” from the Ecoinvent v3.5 database.

In the present work, the construction of set up, manufacturing, transportation, and disposal of wastes based on the raw materials, such as polymers, used in the membrane contactors were not considered for environmental evaluation-based system performance using the LCA methodology. The study has only focused on the process phase indicating CO₂ capture and recovery through both the absorber and the stripping membrane contactors.

It was assumed that the electricity considered as the resource of the energy inputs for both membrane contactors was needed for the absorption and stripping processes, separately. In the absorption membrane contactor, electricity was first required for pumping liquid absorbent from the reservoir to the contactor by Micropump (pump head model GJ-N21-JF1SJ, pump motor model DG-F61.G1T2P5. J. B., Micropump, Vancouver, WA, USA); secondly, it was used during the control of the feed gas flow rate by a multi-channel mass flow controller (model 8248A, Matheson TRI-GAS, Montgomeryville, PA, USA) and mass flow controller transducer (model 8272-0452, Matheson TRI-GAS, Montgomeryville, PA, USA), and finally exposure of the absorbent liquid into the water bath (model HCTB-3020, 12 1 BATH-12, LID-12, Omega Engineering, Stamford, CT, USA) to raise its temperature was another resource for the electricity consumption. In the stripping module, two devices bringing about electricity consumption were considered: one is a vacuum pump (model N810.3 FTP, KNF Neuberger, and Trenton, NJ, USA) applied to strip CO₂ into helium gas, and the other is an oil bath (model HCTB-3030, 26 1 BATH-26, LID-26, Omega Engineering, Stamford, CT, USA) used to heat the absorbent stripped of CO₂.

Calculations were made by considering the amount of electricity consumed during the experiments and taking into account the functional unit of 1kg CO₂ recovery in 1 h within the scope of the LCA methodology; for the hourly electricity consumption calculation, the amperage and voltage information for the devices given above with particular brands and models were found from the catalog published on the websites of the relevant equipment suppliers.

3.3. Life Cycle Impact Assessment

In the present work, three environmental indicators including natural resources, human health, and ecosystems obtained from LCI data were evaluated for life cycle impact assessment. The consumption of energy, materials, and water are considered within natural resources; emissions to air, water, and land are included in ecosystems; finally, emissions of toxic substances from the production of absorbents used in this work are assessed in public health as presented in the previous study conducted by Aldaco and co-workers [60]. The LCA approach was carried out with the commercial software SimaPro v.9 by using ReCiPe Endpoint (H), and ReCiPe Midpoint (H) V1.03 methods. A total of 14 midpoint impact categories are specifically under two endpoints which are ecosystem and human health. The impact categories of ecosystems are ozone formation terrestrial ecosystems potential (OFTEP), terrestrial acidification potential (TAP), freshwater eutrophication potential (FEP), marine eutrophication potential (MEP), terrestrial ecotoxicity potential (TETP), freshwater ecotoxicity potential (FETP), marine ecotoxicity potential (METP). Human health is specifically classified into seven categories including global warming potential (GWP), stratospheric ozone depletion potential (SODP), ionizing radiation potential (IRP), ozone formation human health potential (OFHHP), fine particulate matter formation potential (FPMFP), human carcinogenic toxicity potential (HCTP), and human non-carcinogenic toxicity potential (HNCTP). Since these environmental impact categories have different units, environmental indicators stemming from categories are needed to be normalized to

compare them in terms of effect magnitude and to reveal the relative significance of impact category results [61,62].

4. Results

In this study, the results obtained from many lab-scale CO₂ absorption and stripping experiments using cross-flow hollow fiber polypropylene membrane contactors in aqueous absorbent solutions containing 80%, 90%, and pure MDEA activated by PZ as a reactive absorbent under different operating conditions, such as feed gas flow rate, liquid flow rate, and concentration of the aMDEA absorbent in water to determine the percentage of CO₂ recovered from CO₂ absorption and CO₂ removal rates were evaluated in terms of environmental aspects using LCA methodology. Hence three different feed gas flow rates (FGFR) in the range of 100, 200, and 300 cm³/min; three different liquid flow rates (LFR) changing from 15.10, 16.60, and 18.90 L/h; two different sweep helium flow rates (SHFR) in the range of 50–100 cm³/min; three different solvent concentrations (80%, 90, and pure aMDEA); and only 1 in. Hg (2.54 cm Hg) vacuum on sweep side (VSS) applied were considered to assess the environmental impacts based on both endpoint categories, including human health, ecosystem, and resources, and midpoint categories listed under the subtitle “life cycle impact assessment” above. To evaluate the performance of the processes including absorption and stripping to capture and recover CO₂ from a simulated flue gas environmentally, the percent concentration of CO₂ in the absorber outlet, the percent concentration of CO₂ in the stripper outlet, and CO₂ recovery percent from the ratio between the volumetric rate of stripped CO₂ and the volumetric rate of absorption of CO₂ were taken into consideration (see Tables S2–S4 in the Supplementary Materials).

4.1. The Environmental Impact of Solvent Composition

In the experiments, three solvent compositions including 80 vol% aMDEA/20 vol% water, 90 vol% aMDEA/10 vol% water, and pure aMDEA without water were tested for different operating conditions such as LFRs, FGFRs, and SHFRs to determine CO₂ capture and recovery ratios from a simulated humidified feed gas stream (see Tables S2–S4). To evaluate the environmental impact of solvent concentration both in absorption and stripping processes, three FGFRs in the range of 100–300 cm³/min, one LFR (15.10 L/h), and one VSS value (2.54 cm Hg) were selected in LCA studies. Normalized values of the damage categories under these conditions for the absorption and stripping processes are presented in Figures 3 and 4, respectively.

In addition to results for damage categories, the relative contribution of the absorption and stripping processes to the impact categories standing for the endpoint one for the same conditions are exhibited in Figures 5 and 6, respectively. It can be said that the maximum effect in terms of damage category on absorption and stripping processes is on public health. While FGFR was minimal in the absorption process, the maximum effect on human health was observed in the pure solvent composition, where the solvent concentration was at a maximum. When all the examined conditions are evaluated, it can be easily said that the highest human effect is observed in the case of maximum FGFR and minimum solvent composition (See Figure 3). This can be explained by the remarkable increase in the IRP category, especially when the midpoint impact factors are evaluated (see Figure 5). Ionizing radiation originated from electromagnetic waves or particles that have sufficient energy to initiate atomic ionization damaging cellular molecules like DNA. Hence, it is now recognized to be a significant risk of triggering severe human diseases such as cancer [63,64]. The maximum increase at the IRP impact category observed under with 80% solvent concentration and 300 cm³/min FGFR can be attributed to the increase in the CO₂-loaded solvent at the absorber out because of the decreasing solvent composition.

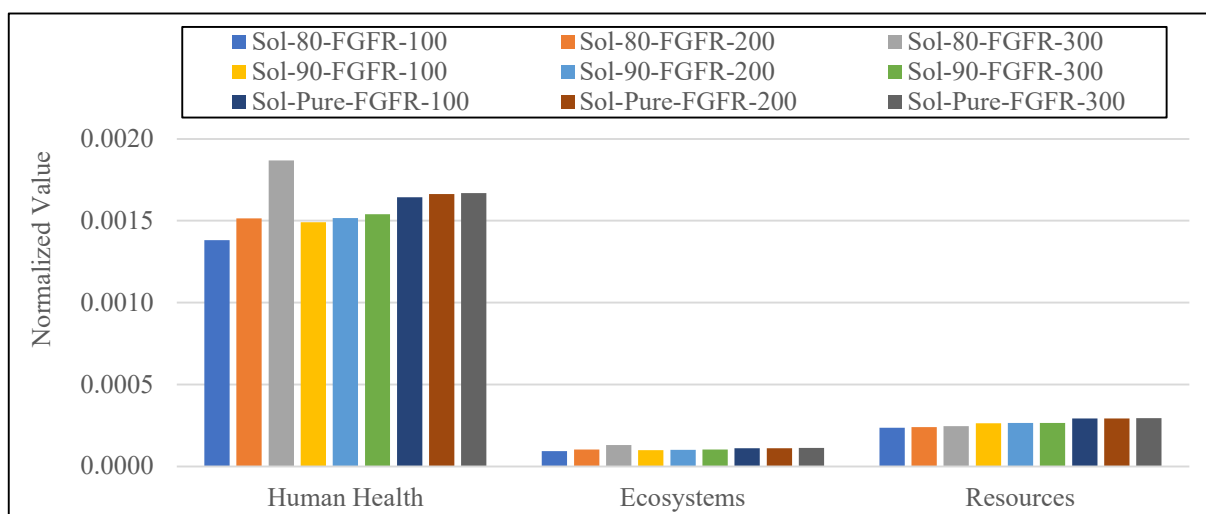


Figure 3. Normalized values of the damage categories for the absorption process at both the three different solvent concentrations, and FGFRs when LFR, SHFR, and VSS were 15.10 L/h, 50 cm³/min, and 2.54 cm Hg, respectively, for all cases. The symbol Sol-80-FGFR-100 stands for solvent (Sol) concentration at 80 vol% aMDEA/20 vol% H₂O and feed gas flow rate (FGFR) at 100 cm³/min.

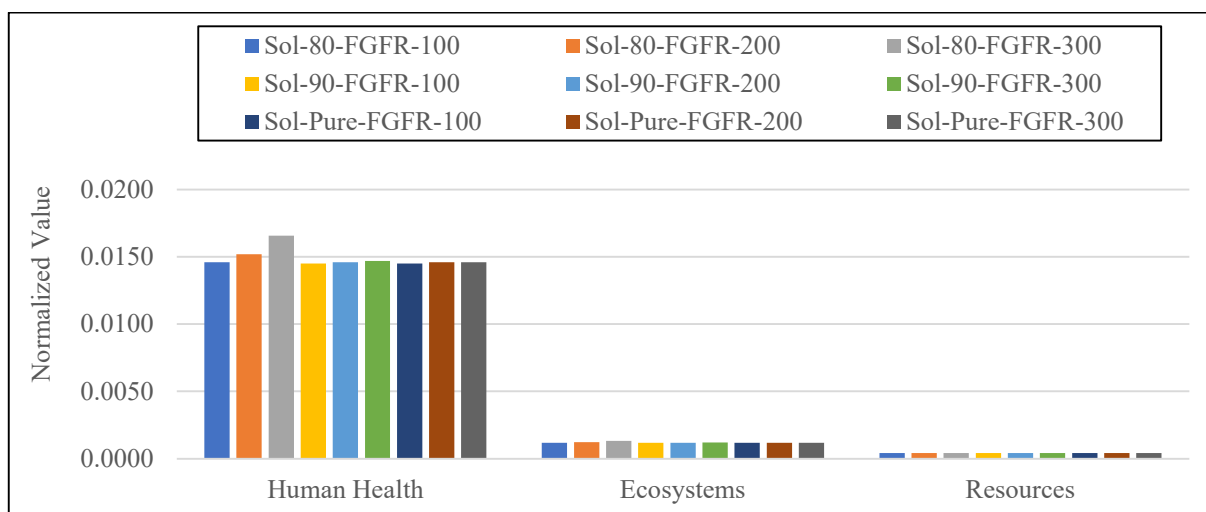


Figure 4. Normalized values of the damage categories for the stripping process at both the three different solvent concentrations, and FGFRs when LFR, SHFR, and VSS were 15.10 L/h, 50 cm³/min, and 2.54 cm Hg, respectively for all cases.

Figure 5 also shows the significant impact observed on FEP for the condition with 80% solvent concentration and 300 cm³/min FGFR. Freshwater eutrophication stemmed from excessive discharges from anthropogenic sources especially agricultural usage of phosphorous fertilizer into the rivers, lakes, and reservoirs has become a global environmental issue. Nutrient over-enrichment, especially phosphorous enrichment is the most significant reason for observing eutrophication in most inland waters. Nutrient enrichment based on urban, agricultural, and industrial improvements has triggered eutrophication, in other words, algal blooms [65,66]. The results for the freshwater eutrophication impact category are considerably different from the results of other impact categories apart from IRP, in other words, it consists of approximately 20% of the total impact on freshwater eutrophication, see Figure 5 [28,67]. This situation is attributed to phosphate emissions from the extraction of fossil fuels. In this study, it can result from the increase in the nitrogen amount at the absorber membrane contactor depending on decreasing solvent concentration.

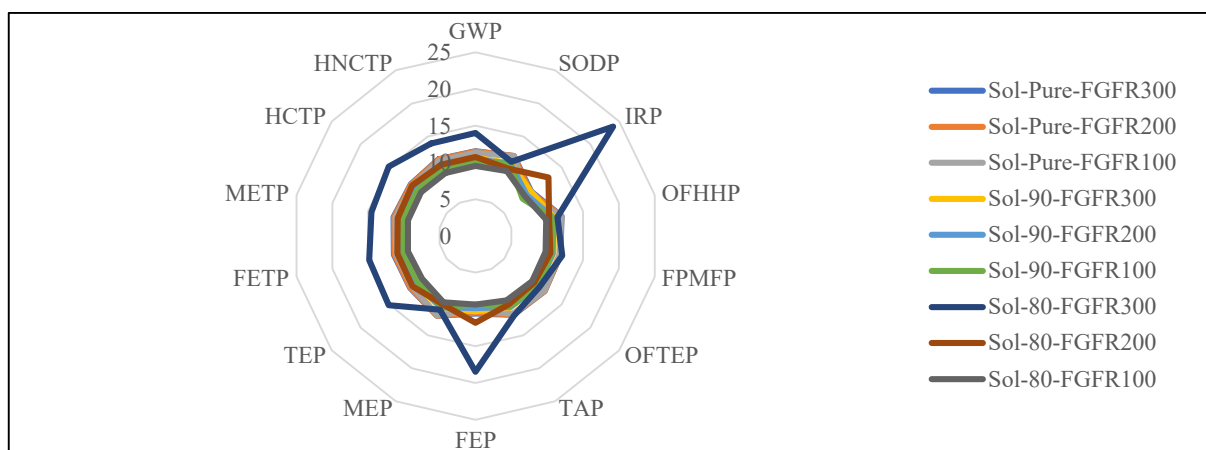


Figure 5. The relative contribution of the absorption process at both the three different solvent concentrations, and FGFRs when LFR, SHFR, and VSS were 15.10 L/h, 50 cm³/min, and 2.54 cm Hg, respectively, for all cases to the impact categories.

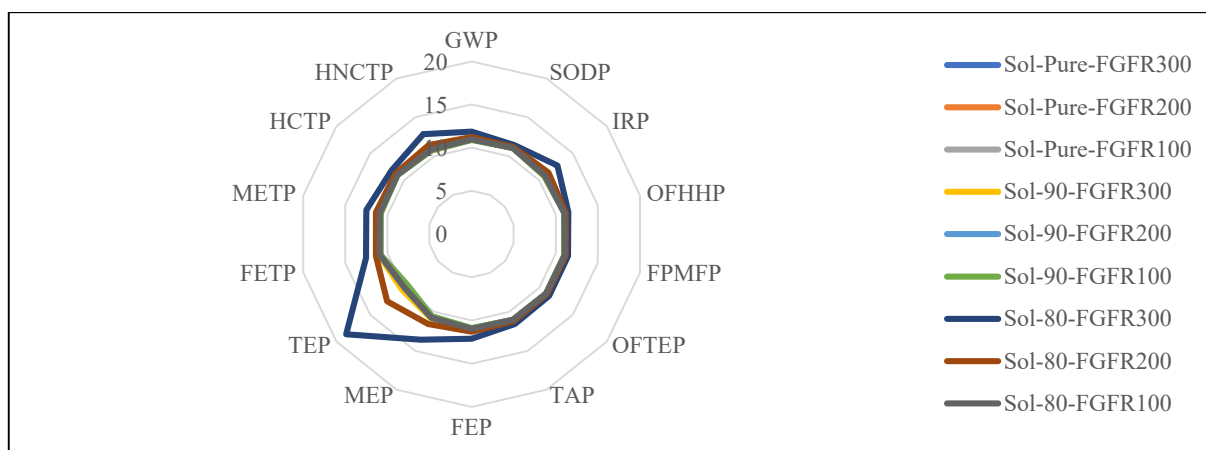


Figure 6. The relative contribution of the stripping process at both the three different solvent concentrations, and FGFRs when LFR, SHFR, and VSS were 15.10 L/h, 50 cm³/min, and 2.54 cm Hg, respectively, for all cases to the impact categories.

In terms of the damage impact category, the stripping contactor had an effect similar to the absorber contactor, and it was determined that the highest effect was on human health. When the environmental effect of the solvent composition in the stripping contactor was evaluated, it was observed that the solvent composition with high composition (90% and pure) had a similar effect in all categories, and when the minimum solvent concentration followed the maximum FGFR, it showed the highest impact as in the absorber contactor (see Figure 4).

In the stripping membrane contactor, TEP revealed a remarkable effect among other endpoint impact categories (see Figure 6). Terrestrial ecotoxicology can be considered as a study related to the impacts of environmental pollutants like pesticides on living organisms including soil microbes, invertebrates, plants, amphibians, reptiles, birds, and mammals in a terrestrial environment like agricultural soil [68,69]. The considerable impact observed in TEP for the lowest solvent concentration and the highest FGFR can be associated with high CO₂-loaded solvent at the stripper.

4.2. The Environmental Impact of Liquid Flow Rate

When the solvent composition and the feed gas flow rate in the system does not change, the environmental effects of different liquid flow rate applications in the absorber

and stripper contactors are examined in terms of damage and impact categories, and the results are shown graphically in Figures 7–10, respectively. In both the absorption and stripping process, it seems that the highest impact is on public health, but in the absorption process, it is followed by resources and the ecosystem, whereas stripping appears to be in the opposite order (see Figures 7 and 8). Once the examined conditions were evaluated in terms of damage categories, it was observed that the different LFR ratios in the stripping process did not show any significant difference in public health, ecosystem, and resources, but the increase in the LFR ratio in the absorption process had a significant impact on public health, which can be associated with the increase in the amount of MDEA and PZ in the absorber contactor, increasing in the IRP category (see Figure 9).

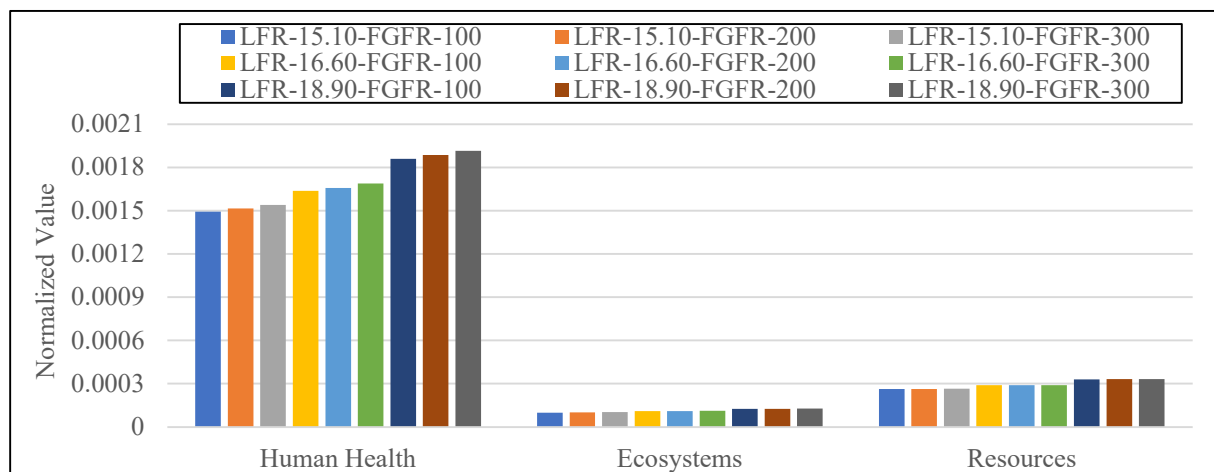


Figure 7. Normalized values of the damage categories for the absorption process at both the three different LFRs, and FGFRs when solvent concentration, SHFR, and VSS were 90 vol% aMDEA/10 vol% H₂O, 50 cm³/min, and 2.54 cm Hg, respectively, for all cases.

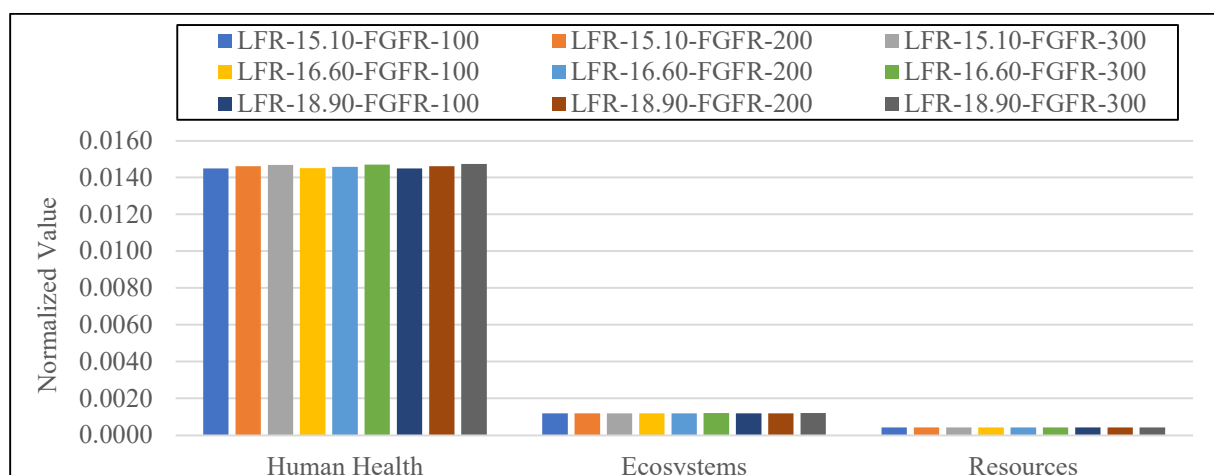


Figure 8. Normalized values of the damage categories for the stripping process at both the three different LFRs, and FGFRs when solvent concentration, SHFR, and VSS were 90 vol% aMDEA/10 vol% H₂O, 50 cm³/min, and 2.54 cm Hg, respectively, for all cases.

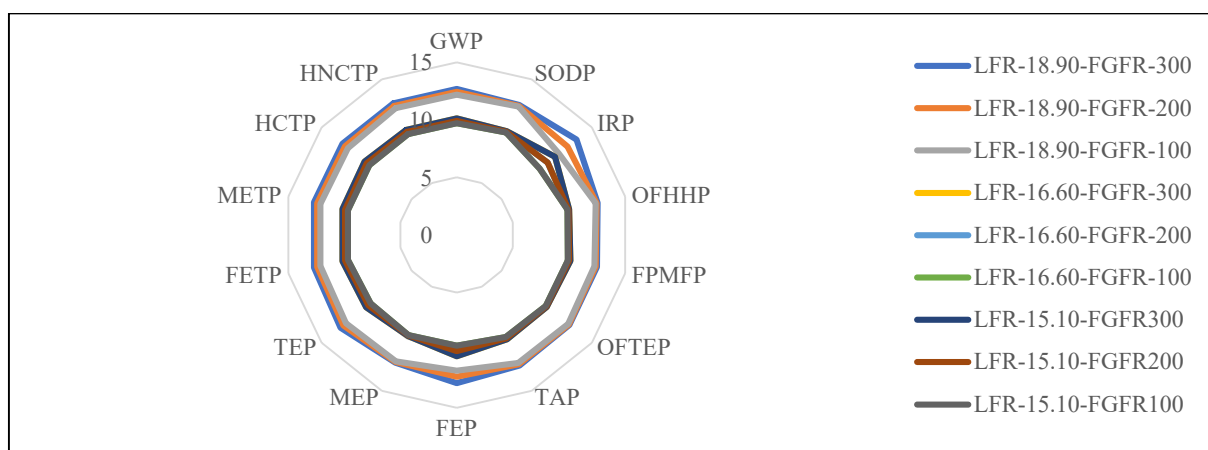


Figure 9. The relative contribution of the absorption process at both the three LFRs, and FGFRs when solvent concentration, SHFR, and VSS were 90 vol% aMDEA/10 vol% H₂O, 50 cm³/min, and 2.54 cm Hg, respectively, for all cases to the impact categories.

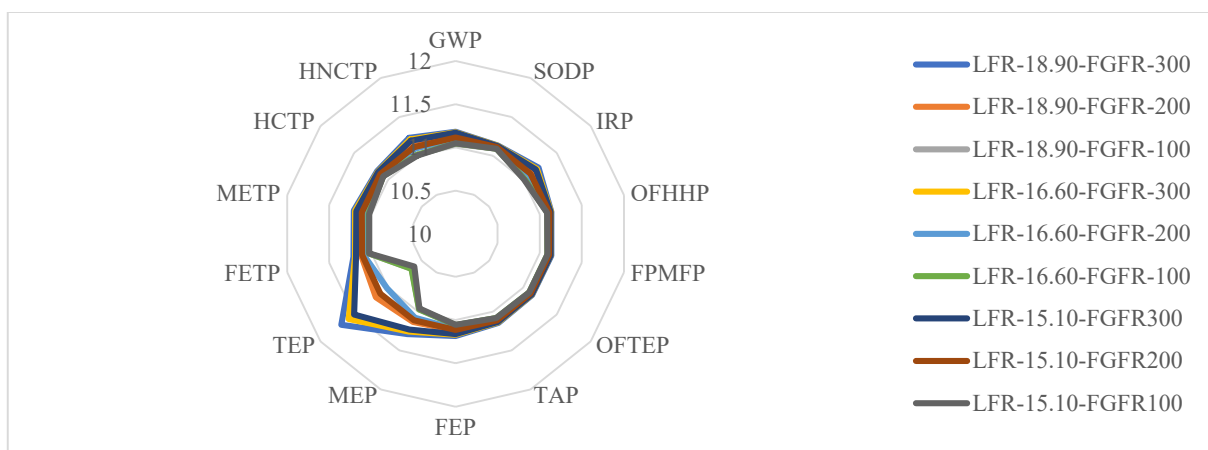


Figure 10. The relative contribution of the stripping process at both the three LFRs, and FGFRs when solvent concentration, SHFR, and VSS were 90 vol% aMDEA/10 vol% H₂O, 50 cm³/min, and 2.54 cm Hg, respectively, for all cases to the impact categories.

In general, it can be concluded that the decrease in LFR in the absorption and stripping processes causes a decrease in all impact categories. When the solvent composition is 90% and the SHFR ratio is 50 cm³/min, and the GWP impacts based on the absorption and stripping processes are compared, the maximum value is calculated as 18.25 and 28.19 kg CO₂ eq for the conditions where LFR and FGFR are at a maximum for the absorption and stripping processes, respectively. The climate system consists of the atmosphere, hydrosphere, biosphere, and geosphere and also their interactions physically, chemically, and biologically with each other [70]. Anthropogenic emissions, such as CO₂ and other greenhouse gases caused by human activities have contributed to global warming that has a direct effect on the temperature of the atmosphere and oceans. The increase in atmospheric temperature leads to some extreme meteorological events, such as sea level rise and extreme heat that have negative social and ecological impacts on human health and the world's ecosystems [71]. The decrease in GWP due to the decrease in LFR observed in the absorption and stripping process can be associated with the decrease in CO₂ gas at the outlet of the absorber and stripper contactors. The remarkable difference in GWP values resulting from absorption and stripping processes can be explained by the fact that much more energy is needed for the stripping process.

The human toxicity potential was mentioned for the first time by Guinée and Heijungs (1993) [72] to express the potential harm of a compound released into the environment on public health [72,73]. Human toxicity is used to weigh emissions inventoried as a part of an LCA by evaluating their impacts, such as carcinogens and non-carcinogens [73]. For the human toxicity impact category including HCTP and HNCTP, the results show that the highest LFR has the highest environmental impact because of the toxic byproducts produced during the manufacturing of solvents used in the experiments. When damage categories are evaluated in terms of impact in stripping processes, the impact of LFR change on resources is much lower than the impact on the ecosystem. Here, it can be said that the effect observed in the ecosystem is similarly related to OFTEP, TAP, FEP, MEP, FETP, and MEP, but TEP is slightly more effective (see Figure 10).

Terrestrial acidification resulting from the atmospheric deposition of acidifying compounds like nitrogen oxides (NO_x), ammonia (NH_3), and sulfur dioxide (SO_2) as a result of human activities brings about direct and indirect severe impacts on ecosystems [74–76]. The increase in nitrogen and sulfur deposition leads to a decrease in the soil's solution pH that triggers some negative consequences in terrestrial ecosystems, such as the extinction of some plant species, and alterations in biotic community structure and composition [75,76]. The results in the present study for the terrestrial acidification impact category exhibit an increasing trend in SO_2 equivalents concerning increasing LFR for both two processes.

4.3. The Environmental Impact of Feed Gas Flow Rate

If the experimental conditions are as follows: the solvent concentration of 100% aMDEA; SHFR $50 \text{ cm}^3/\text{min}$; LFR of 15.10, 16.60, and 18.90 L/h ; and FGFR of 100, 200, and $300 \text{ cm}^3/\text{min}$, the environmental impact of FGFR in terms of damage and impact categories on the absorber and the stripper contactor are as presented in Figures 11–14, respectively. Normalized values of damage categories for both absorption and stripping processes under the examined circumstances revealed that the differences in FGFR do not have any significant impact on human health, demonstrating the highest impact based on the process, ecosystem, and resources (see Figures 11 and 12).

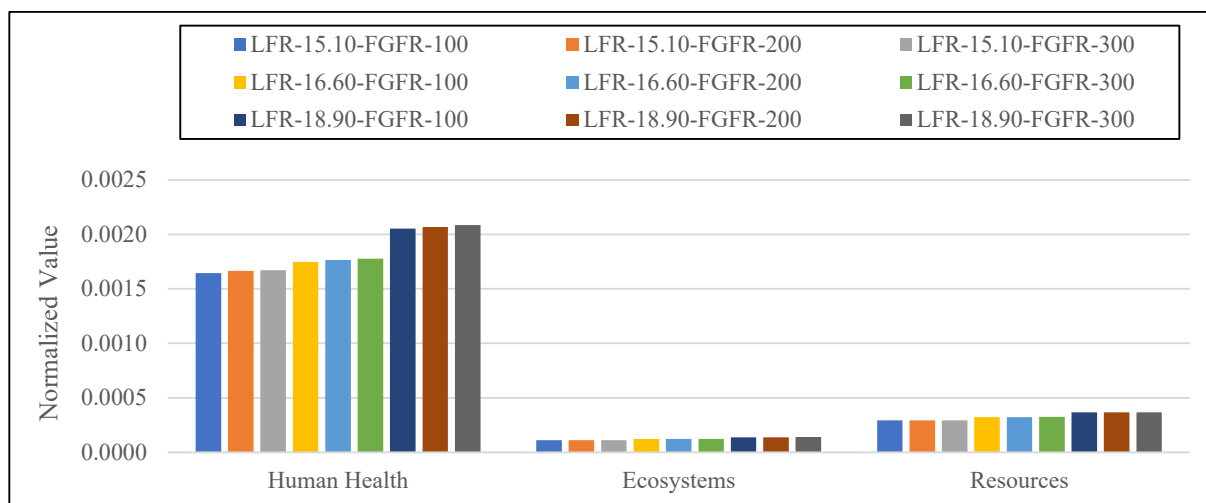


Figure 11. Normalized values of the damage categories for the absorption process at both the three different LFRs, and FGFRs when solvent concentration, SHFR, and VSS were pure, $50 \text{ cm}^3/\text{min}$, and 2.54 cm Hg , respectively, for all cases.

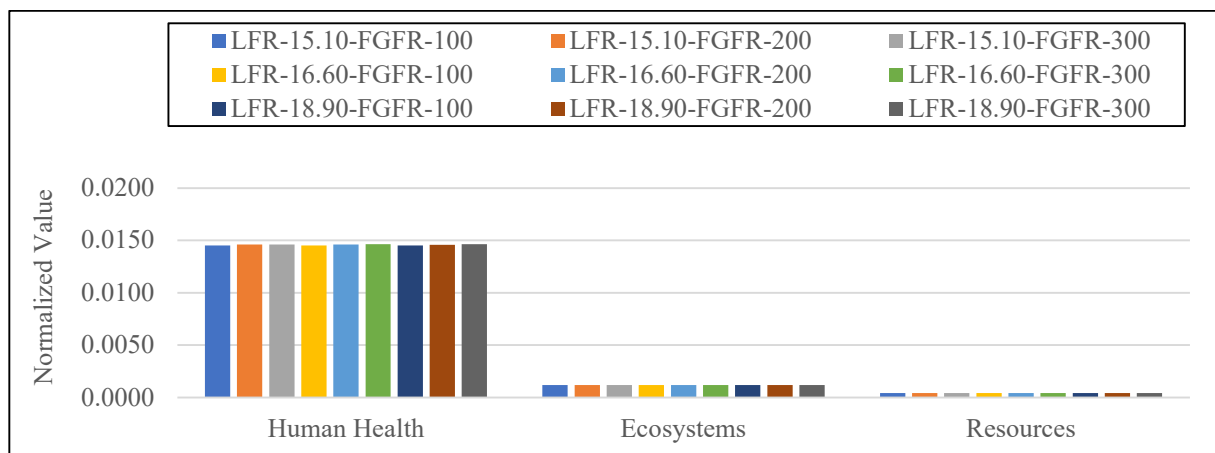


Figure 12. Normalized values of the damage categories for the stripping process at both the three different LFRs, and FGFRs when solvent concentration, SHFR, and VSS were pure, 50 cm³/min, and 2.54 cm Hg, respectively, for all cases.

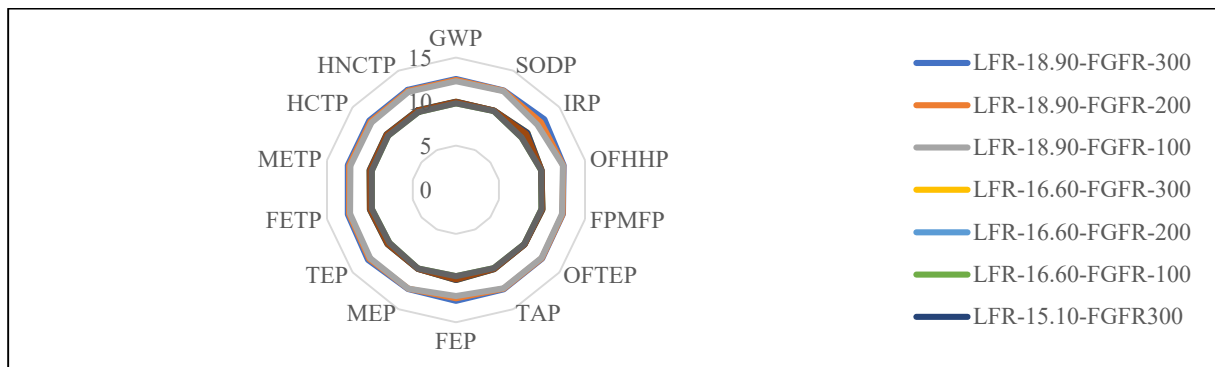


Figure 13. The relative contribution of the absorption process at both the three LFRs, and FGFRs when solvent concentration, SHFR, and VSS were pure, 50 cm³/min, and 2.54 cm Hg, respectively, for all cases to the impact categories.

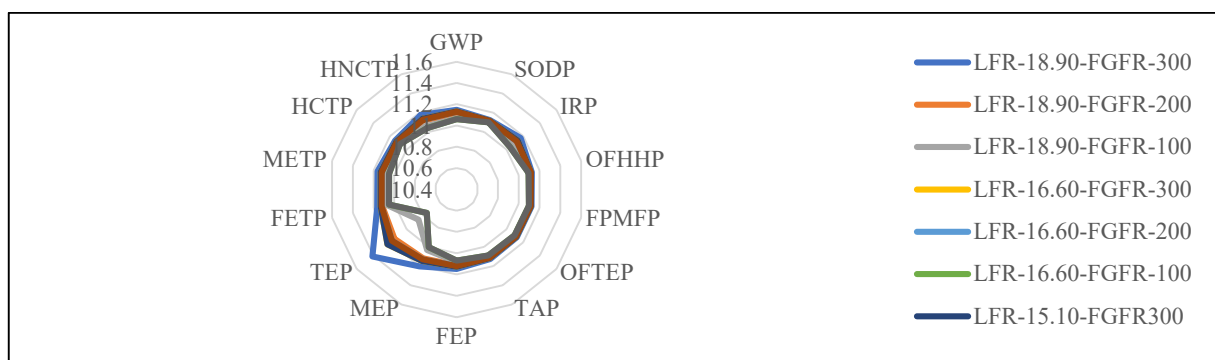


Figure 14. The relative contribution of the stripping process at both the three LFRs, and FGFRs when solvent concentration, SHFR, and VSS were pure, 50 cm³/min, and 2.54 cm Hg, respectively, for all cases to the impact categories.

The ozone layer surrounding the earth's surface protects the earth against the harmful ultraviolet rays from the sun by absorbing, especially, most ultraviolet B (UV-B) radiation that leads to some illnesses, such as cataracts, deformation of eye lenses, and skin cancer from of exposure to the huge amount of UV-B radiation. In addition to these effects on public health, excessive UV-B radiation diminishes the rates of plant growth and the

balance of the ecosystems alters [77,78]. Stratospheric ozone depletion resulting from ozone-depleting substance (ODS) emissions like halocarbons consisting of both carbon and at least one of the halogens (fluorine, chlorine, iodine, and bromine) is of vital importance as an environmental threat to both the anthroposphere and the biosphere [77,79]. In this context, SODP is a significant parameter to assess the impacts of ODS on stratospheric ozone [80].

In the present study, considering SODP in absorption (2.12×10^{-5} kg CFC11 eq) and stripping (1.70×10^{-5} kg CFC11 eq) processes, it reached the highest impact under conditions where the solvent composition was at a minimum and LFR and FGFR were at the maximum.

Particulate matter with an aerodynamic diameter less than or equal to $2.5 \mu\text{m}$ ($\text{PM}_{2.5}$) that has a severe impact on climate change and public health is attributed to two sources: one based on natural sources including sea salt, dust, forest, and grassland fires and the second based on anthropogenic sources comprising power plants, industrial processes, and vehicular exhaust as well as emissions from residential activities [81–83]. While it was understood that FGFR was not effective on FPMFP in absorption and stripping processes, the maximum effect was found to be 0.042 and 0.047 kg $\text{PM}_{2.5}$ eq for absorption and stripping processes, respectively, when the solvent composition reached the minimum, and LFR and FGFR reached the maximum, similar to SODP.

4.4. The Environmental Impact of Sweep Gas Flow Rate

In the experiments, helium was used as a sweep gas at the stripper side in the range of $50\text{--}100 \text{ cm}^3/\text{min}$. To determine the environmental impact based on SHFR, normalized values of damage categories and the relative contribution of the stripping process with the solvent concentration of 80 vol% aMDEA/20 vol% H_2O and VSS of 2.54 cm Hg to the impact categories are presented in Figures 15 and 16, respectively. It is deduced from Figure 15 that as SHFR increases, the impact on public health and the ecosystem decreases, and the impact on resources, on the contrary, increases. This effect on public health and ecosystems can be explained by the decrease in CO_2 at the outlet of the stripper contactor with the increase in the SHFR feeding into the stripper.

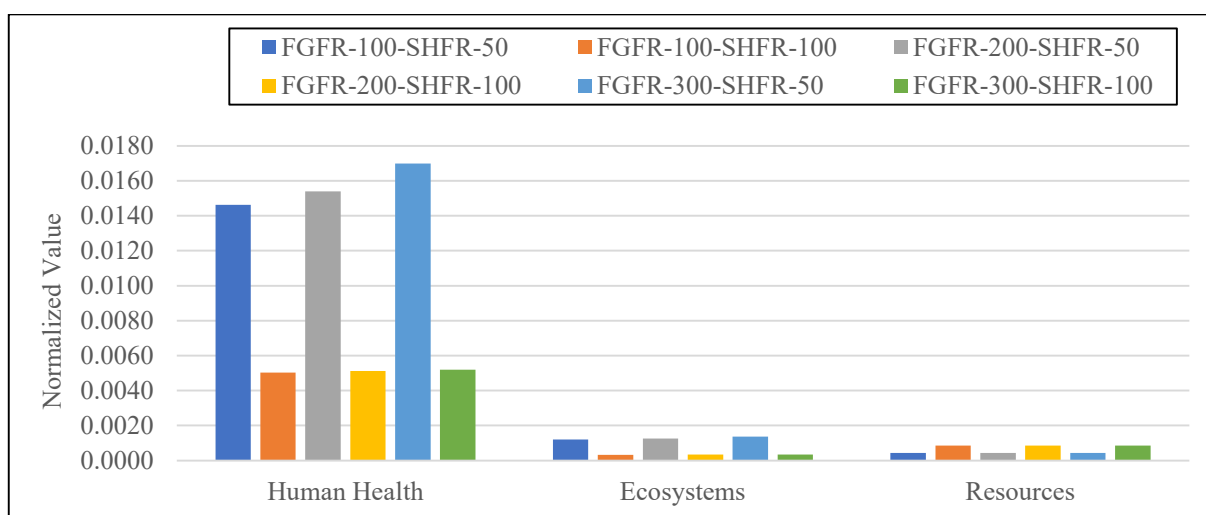


Figure 15. Normalized values of the damage categories for the stripping process at three different FGFRs, and two different SHFRs, when solvent concentration, LFR, and VSS were 80 vol% aMDEA/20 vol% H_2O , 18.90 L/h, and 2.54 cm Hg, respectively, for all cases.

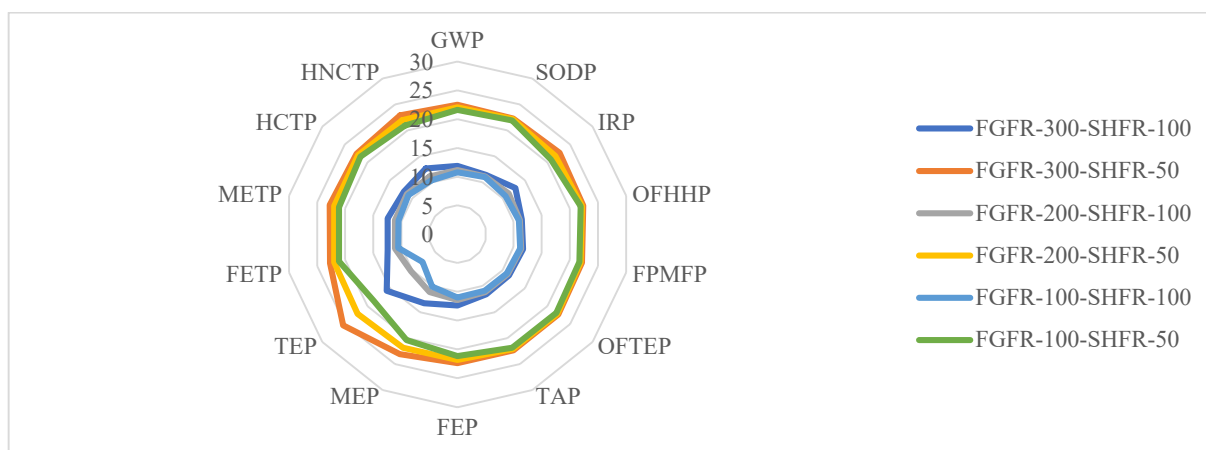


Figure 16. The relative contribution of the stripping process at three different FGFRs, and two different SHFRs, when solvent concentration, LFR, and VSS were 80 vol% aMDEA/20 vol% H₂O, 18.90 L/h, and 2.54 cm Hg, respectively, for all cases to the impact categories.

Since some organisms living in estuarine and coastal zones are more sensitive than freshwater organisms towards environmental contaminants, such as surfactants that can give rise to irreversible long-term impacts due to their accumulation in remarkable concentrations, marine environments are considered sensitive ecosystems [84]. In the current study, the highest effect on METP was observed under the condition with the maximum FGFR and the minimum SHFR (see Figure 16).

Evaluation of the ecotoxicological impacts of environmental pollutants from various sources on freshwater ecosystems is of vital significance in terms of environmental risk assessment [85]. In the assessment of the ecotoxicity potential of the contaminants emitted into freshwater locations, regional properties of the ecosystem, such as the chemical composition of the water body and species diversity should be taken into account because of regional differences in the relationship between freshwater and toxic substances [86]. The results related to the freshwater ecotoxicity impact category for all concepts showed that the stripping membrane contactors performed with the lowest SHFR and solvent composition, and the highest FGFR and LFR are of the highest significance. Koornneef et al. (2008) [37] explained the reason for FETP as discharging of emissions of metals into the receiving environment like water (river and groundwater) and air.

Compounds including excessive nutrients are discharged into the marine environment in two ways: (i) point sources expressing industrial waters and municipal sewage sludges and (ii) non-point sources originating from diffuse sources, such as urban and agricultural runoff, groundwater transport, and atmospheric inputs by dry or wet deposition. As a result of these types of discharges, marine waters will enrich in terms of organic and inorganic materials bringing about marine eutrophication [87]. Considering marine eutrophication potential in the present study, the results showed that as in all other impact categories, the effect is higher in the case of low SHFR.

5. Discussion

CO₂ is one of the major greenhouse gases and remarkably its concentration in the atmosphere is increasing annually, leading to a global impact on the environment, economy, and society. A technology with minimum environmental impact and high CO₂ capture capacity should be preferred in the selection of methods to be applied to reduce greenhouse gases in the atmosphere.

To the best of our knowledge, this study can be regarded as the first published LCA for post-combustion CO₂ capture and recovery by pure aMDEA in crossflow membrane contactors having coated hollow fibers. Hence, the present study will hopefully contribute to filling this gap in the literature. The goal of the present work was to evaluate the

environmental impacts of a process called membrane gas absorption, which both includes chemical absorption of CO₂ with aqueous MDEA activated by PZ and the usage of the hollow fiber PP membranes as a non-selective barrier. This process is one of the most promising options among these alternatives owing to its advantages, such as a larger gas–liquid interfacial area, easier scale-up, and independent phase interactions in comparison with conventional techniques like packed towers [17,88]. To evaluate the environmental impact based on different operating conditions used in a membrane–gas absorption process for post-combustion CO₂ capture and recovery by pure aMDEA in crossflow membrane contactors having coated hollow fibers, the present study assumed to recover of 1 kg CO₂ within 1 h as a functional unit. Hence, all assessments were implemented based on this assumption. Results investigating the impacts of various operating conditions performed during the experiments, including solvent composition ratio, LFR, FGFR, and SHFR, revealed that although FGFR did not have a remarkable effect in terms of damage and impact categories, it was found that the change in the solvent concentration, together with the change in LFR and SHFR ratios, affected public health and ecosystem, and therefore on the related midpoint categories. It can be said that the outstanding effects among the impact categories are especially related to IRP and TEP. The total effects associated with the midpoint categories resulting from absorption and stripping processes are presented in Tables 1 and 2 for SHFR 50 cm³/min and 100 cm³/min, respectively, whereas FGFR is at the maximum, and solvent composition and LFR changes. Moreover, absolute values of the impact categories and damage categories for different operating conditions are presented in Tables S5–S12 in the Supplementary Materials, respectively.

Table 1. Absolute values of the impact categories at three different LFRs, and solvent compositions when FGFR, SHFR, and VSS were 300 cm³/min, 50 cm³/min, and 2.54 cm Hg.

Impact Category	Unit	Sol-Pure-LFR-18.90	Sol-90-LFR-18.90	Sol-80-LFR-18.90	Sol-Pure-LFR-15.10	Sol-90-LFR-15.10	Sol-80-LFR-15.10
GWP	kg CO ₂ eq	46.44	45.09	50.13	42.67	41.66	45.76
SODP	kg CFC11 eq	3.95×10^{-5}	3.72×10^{-5}	3.75×10^{-5}	3.47×10^{-5}	3.31×10^{-5}	3.34×10^{-5}
IRP	kBq Co-60 eq	3.055	3.045	5.095	2.780	2.790	4.448
OFHHP	kg NO _x eq	0.134	0.127	0.129	0.118	0.113	0.115
FPMFP	kg PM _{2.5} eq	0.087	0.083	0.087	0.079	0.076	0.079
OFTEP	kg NO _x eq	0.157	0.149	0.149	0.138	0.131	0.132
TAP	kg SO ₂ eq	0.201	0.192	0.202	0.179	0.171	0.180
FEP	kg P eq	0.0134	0.013	0.0176	0.0124	0.0123	0.0158
MEP	kg N eq	0.0059	0.0054	0.0054	0.0048	0.0044	0.0045
TEP	kg 1,4-DCB	73.19	70.03	89.73	60.82	58.64	74.74
FETP	kg 1,4-DCB	0.934	0.900	1.075	0.833	0.809	0.953
METP	kg 1,4-DCB	1.367	1.315	1.549	1.217	1.179	1.373
HCTP	kg 1,4-DCB	1.546	1.506	1.747	1.421	1.392	1.591
HNCTP	kg 1,4-DCB	27.22	26.02	30.24	23.92	23.03	26.51

Table 2. Absolute values of the impact categories at three different LFRs, and solvent compositions when FGFR, SHFR, and VSS were 300 cm³/min, 100 cm³/min, and 2.54 cm Hg.

Impact Category	Unit	Sol Pure-LFR-18.90	Sol-90-LFR-18.90	Sol-80-LFR-18.90	Sol-Pure-LFR-15.10	Sol-90-LFR-15.10	Sol-80-LFR-15.10
GWP	kg CO ₂ eq	73.93	72.68	81.17	70.21	69.34	75.61
SODP	kg CFC11 eq	5.55×10^{-5}	5.34×10^{-5}	5.45×10^{-5}	5.08×10^{-5}	4.92×10^{-5}	4.99×10^{-5}
IRP	kBq Co-60 eq	4.539	4.551	7.137	4.277	4.316	6.226
OFHHP	kg NO _x eq	0.189	0.183	0.189	0.174	0.168	0.173
FPMFP	kg PM _{2.5} eq	0.129	0.126	0.133	0.121	0.119	0.124
OFTEP	kg NO _x eq	0.217	0.208	0.213	0.197	0.190	0.194
TAP	kg SO ₂ eq	0.291	0.282	0.298	0.268	0.262	0.274
FEP	kg P eq	0.0206	0.0205	0.0262	0.0197	0.0196	0.0238
MEP	kg N eq	0.0064	0.0059	0.0061	0.0053	0.0049	0.0051
TEP	kg 1,4-DCB	95.27	92.47	134.95	83.12	81.47	112.81
FETP	kg 1,4-DCB	1.362	1.331	1.609	1.263	1.242	1.447
METP	kg 1,4-DCB	1.985	1.937	2.315	1.838	1.805	2.084
HCTP	kg 1,4-DCB	2.4286	2.392	2.743	2.305	2.281	2.541
HNCTP	kg 1,4-DCB	38.14	37.02	44.32	34.88	34.09	39.47

When Tables 1 and 2 are evaluated together, low SHFR showed a lower effect in all categories associated with low helium gas fed to the stripping process. Considering the impact categories one by one, the minimum effect was observed in most of the categories when the solvent composition was 90% and the LFR was 15.10 L/h, but in some categories, the minimum effect or values very close to the minimum were determined in cases where the solvent composition was pure. On the contrary, it was determined that the magnitude in many impact categories, including GWP, IRP, FPMFP, FEP, TEP, FETP, METP, HCTP, HNCTP, reached the maximum for the conditions where the solvent composition was at the minimum and the LFR was maximum.

The previous studies evaluated the environmental impact of post-combustion CO₂ capture based on membrane separation [21,28,30]. Troy et al., 2016 [30] analyzed 13 different power plant concepts with and without CCS using the LCA methodology. The concepts considered in the study represent state-of-the-art technologies in both, the power plant sector and CCS, covering post-combustion, oxyfuel, and pre-combustion concepts. Classic CCS concepts are compared for the first time with approaches using newly emerging membrane technologies. Power plant concepts without CCS were considered reference cases. The concepts using integrated gasification combined cycle led to overall better results.

Giordano et al., 2018 [28] aimed to compare life cycle emissions of membrane separation and chemical absorption processes for the post-combustion capture of one tonne of CO₂ from a subcritical coal-fired power plant using the LCA methodology. The greatest reduction potential was observed for human toxicity and impacts on freshwater and marine ecosystems, because of the elimination of environmental concerns related to solvent manufacturing and disposal of amine reclaimer wastes. Khaki et al., 2021 [21] analyzed the life cycle assessment of polymeric membranes, namely polyacrylonitrile (PAN), polyvinylimidazole (PVIM), and copolymer P(AN-co-VIM): 50:50 ratio utilized for CO₂ sequestration. They concluded that the remarkable environmental impacts based on the synthesis of the PVIM membrane, which was figured out to be the most adapted to environmental regulations, were associated with global warming (118.42 kg CO₂ eq), marine ecotoxicity (15712.82 kg 1,4-DB eq), and human toxicity (67.285 kg 1,4-DB eq) categories due to the DMF discharge and electricity demand. The current study did not take into account the manufacturing-based factors such as the extraction of the raw material and the synthesis

of the membrane. Since it is the first study aimed at determining the conditions that will keep the environmental damage to a minimum during the capture and recovery of post-combustion CO₂ at the process scale, it reveals differences from the results of the life cycle assessment of the processes presented in the previous studies. The current study aimed to show that environmental impacts particularly based on an energy-intensive stripping process can be reduced in the case of the usage of pure aMDEA solvent concentration. Correspondingly, future works should compare the environmental impacts in the diverse operating circumstances of technologies preferred to capture and recover CO₂ from feed gas steam and identify their further improvement alternatives to reduce specific energy requirements needed for pumping of liquid contributing significantly to environmental impacts as well as to diminish the solvent impact. Moreover, for further investigations, considering the application of the study on the pilot scale, it is advisable to choose solvent types with lower viscosity and more cost-effective operating conditions in terms of energy efficiency and environmental aspects. In addition to these recommendations for future works, important errors during the experiments can result from the lack of amine strength measurements which determine the working capacity of the absorbent liquid that was performed in the present study. Hence, it is recommended to perform regeneration tests in future studies to ensure the amine concentration in the reservoir.

6. Conclusions

The focus of this study is to determine the operating conditions that will provide the most environmentally friendly approach to recovering 1 kg of CO₂ per hour by utilizing the LCA methodology. Simulation results pointed out that life cycle emissions of post-combustion CO₂ capture and recovery from a simulated humidified feed gas by a membrane gas absorption process were associated with the concentration of solvents, liquid flow rates, and sweep helium gas flow rate, whereas feed gas flow rate did not have any significant impact. As expected, an increase in the amount of CO₂ at the outlet of the absorber and stripper due to the decrease in solvent concentration, increase in LFR, and increase in SHFR can cause an increase in the magnitude of the damage and impact categories. These simulation results demonstrated consistency with the experimental results performed for pure aMDEA condition, which has a much lower absorbent circulation load, eliminates the energy needed to heat and evaporate water present in aqueous absorbent solutions, and benefits from the absence of excess water during the stripping [51].

The most remarkable contributors to impact categories are absorbents used in the chemical absorption of CO₂ and helium gas used in the stripping process as well as the electricity needed for pumping liquid absorbent from the reservoir to the gas separation tank and turning on the devices used during the experiments. The absolute values of impact categories covering both absorption and stripping processes indicated that the ionizing radiation (7.137 kBq Co-60 eq) potential represented the most significant environmental impact followed by the freshwater eutrophication (0.0262 kg P eq) potential and terrestrial ecotoxicity (134.95 kg 1,4-DCB) potential due to the usage of aqueous solvents including MDEA and PZ, and electricity consumption. The study highlights the importance of LCA in the determination of environmentally more sustainable process conditions during the recovery of CO₂ with aqueous aMDEA solution using a compact hollow fiber device for the absorber as well as the stripper. It is noted that the present work did not take into account construction, transportation, maintenance phases, and final disposal of wastes, it only focused on the process stage. Therefore, future efforts in the evaluation of the environmental impacts of the system would need to focus on LCA methodology containing a system boundary based on the “from cradle to grave” approach to decide which condition is more environmentally friendly.

Supplementary Materials: The following supporting information can be downloaded at: <https://www.mdpi.com/article/10.3390/atmos14030490/s1>, Table S1: Inventory data for 1 kgCO₂/h (recovered) via cross-flow hollow fiber PP membrane contactor in aMDEA absorbent solution; Table S2: CO₂ absorption/stripping results in aMDEA absorbent composition of 80 vol% aMDEA/10 vol% H₂O; Table S3: CO₂ absorption/stripping results in aMDEA absorbent composition of 90 vol% aMDEA/10 vol% H₂O; Table S4: CO₂ absorption/stripping results with pure aMDEA; Table S5: Absolute values of the impact categories for different LFR and FGFR at the pure solvent composition and 50 cm³/min of SHFR; Table S6: Absolute values of the impact categories for different LFR and FGFR at the pure solvent composition and 100 cm³/min of SHFR; Table S7: Absolute values of the impact categories for different LFR and FGFR at the 90% of solvent composition and 50 cm³/min of SHFR; Table S8: Absolute values of the impact categories for different LFR and FGFR at the 90% of solvent composition and 100 cm³/min of SHFR; Table S9: Absolute values of the impact categories for different LFR and FGFR at the 80% of solvent composition and 50 cm³/min of SHFR; Table S10: Absolute values of the impact categories for different LFR and FGFR at the 80% of solvent composition and 100 cm³/min of SHFR; Table S11: Absolute values of the damage categories for different solvent composition, LFR, FGFR at 50 cm³/min of SHFR; Table S12: Absolute values of the damage categories for different solvent composition, LFR, FGFR at 100 cm³/min of SHFR.

Author Contributions: Conceptualization, A.P.A.; methodology, A.P.A.; literature review, A.P.A.; analytics and data curation, A.P.A.; writing—original draft preparation, A.P.A.; writing—review and editing, all authors; supervision, G.G. and K.K.S. All authors have read and agreed to the published version of the manuscript.

Funding: This research was funded by The Scientific and Technological Research Council of Turkey (TUBITAK)-2214A.

Institutional Review Board Statement: Not applicable.

Informed Consent Statement: Not applicable.

Data Availability Statement: Not applicable.

Acknowledgments: Data used in the current study are taken from the first author's Ph.D. thesis. Aytac Perihan Akan was financially supported by The Scientific and Technological Research Council of Turkey (TUBITAK) with 2214A-fellowship to implement her studies at the fourth author's laboratory under his co-supervision at the New Jersey Institute of Technology (NJIT), Department of Chemical and Materials Engineering, Newark, NJ, USA.

Conflicts of Interest: The authors declare no conflict of interest.

Nomenclature

aMDEA	Activated methyldiethanolamine
CCS	Carbon capture and storage
FEP	Freshwater eutrophication potential
FETP	Freshwater ecotoxicity potential
FGFR	Feed gas flow rates
FPMFP	Fine particulate matter formation potential
GWP	Global warming potential
HCTP	Human carcinogenic toxicity potential
HNCTP	Human non-carcinogenic toxicity potential
IRP	Ionizing radiation potential
LCA	Life cycle assessment
LFR	Liquid flow rates
MDEA	Methyldiethanolamine
MEP	Marine eutrophication potential
METP	Marine ecotoxicity potential
OFHHP	Ozone formation human health potential
OFTEP	Ozone formation terrestrial ecosystem potential
PZ	Piperazine
SHFR	Sweep helium flow rates

SODP	Stratospheric ozone depletion potential
TAP	Terrestrial acidification potential
TEP	Terrestrial ecotoxicity potential
VSS	Vacuum on the sweep side

References

1. Brandão, M.; Levasseur, A.; Kirschbaum, M.U.F.; Weidema, B.P.; Cowie, A.L.; Jørgensen, S.V.; Hauschild, M.Z.; Pennington, D.W.; Chomkamsri, K. Key issues and options in accounting for carbon sequestration and temporary storage in life cycle assessment and carbon footprinting. *Int. J. LCA* **2013**, *18*, 230–240. [CrossRef]
2. Powell, C.E.; Qiao, G.G. Polymeric CO₂/N₂ gas separation membranes for the capture of carbon dioxide from power plant flue gases. *J. Membr. Sci.* **2006**, *279*, 1–49. [CrossRef]
3. Wang, Y.; Pan, Z.; Zhang, W.; Borhani, T.N.; Li, R.; Zhang, Z. Life cycle assessment of combustion-based electricity generation technologies integrated with carbon capture and storage: A review. *Environ. Res.* **2022**, *207*, 112219. [CrossRef] [PubMed]
4. Chen, C.; Yang, S. The energy demand and environmental impacts of oxy-fuel combustion vs. post-combustion capture in China. *Energy Strategy Rev.* **2021**, *38*, 100701. [CrossRef]
5. Chisalita, D.A.; Petrescu, L.; Cobden, P.; van Dijk, H.E.; Cormos, A.M.; Cormos, C.C. Assessing the environmental impact of an integrated steel mill with post-combustion CO₂ capture and storage using the LCA methodology. *J. Clean. Prod.* **2019**, *211*, 1015–1025. [CrossRef]
6. Fang, J.; Jin, X.; Huang, K. Life cycle analysis of a combined CO₂ capture and conversion membrane reactor. *J. Membr. Sci.* **2018**, *549*, 142–150. [CrossRef]
7. Iliuta, I.; Bougie, F.; Iliuta, M.C. CO₂ Removal by Single and Mixed Amines in a Hollow-Fiber Membrane Module-Investigation of Contactor Performance. *AIChE J.* **2015**, *61*, 955–971. [CrossRef]
8. Da Cruz, T.T.; Balestieri, J.A.P.; de Toledo Silva, J.M.; Vilanova, M.R.; Oliveira, O.J.; Ávila, I. Life cycle assessment of carbon capture and storage/utilization: From current state to future research directions and opportunities. *Int. J. Greenh. Gas Control* **2021**, *108*, 103309. [CrossRef]
9. Wang, M.; Joel, A.S.; Ramshaw, C.; Eimer, D.; Musa, N.M. Process intensification for post-combustion CO₂ capture with chemical absorption: A critical review. *Appl. Energy* **2015**, *158*, 275–291. [CrossRef]
10. Zhao, S.; Feron, P.H.M.; Deng, L.; Favre, E.; Chabanon, E.; Yan, S.; Hou, J.; Chen, V.; Qi, H. Status and progress of membrane contactors in post-combustion carbon capture: A state-of-the-art review of new developments. *J. Membr. Sci.* **2016**, *511*, 180–206. [CrossRef]
11. National Oceanic and Atmospheric Administration (NOAA). 2022. Available online: https://gml.noaa.gov/ccgg/trends/gl_trend.html (accessed on 1 June 2022).
12. International Energy Agency (IEA). CO₂ Emissions from Fuel Combustion Overview. 2018. Available online: <https://www.iea.org/subscribe-to-data-services/co2-emissions-statistics> (accessed on 7 February 2021).
13. International Energy Agency (IEA). Global Energy Review 2021. 2021. Available online: <https://www.iea.org/reports/global-energy-review-2021/co2-emissions> (accessed on 8 June 2022).
14. Ahmed, A.A.J.; Alias, M.; Ahmed, D.S.; Abdallah, M.; Bufaroosha, M.; Jawad, A.H.; Yousif, E. Investigating CO₂ storage properties of Pd (II) and Co (II) chelates of a Schiff's base ligand. *J. Umm Al-Qura Univ. Appl. Sci.* **2023**, 1–9. [CrossRef]
15. Albo, J.; Luis, P.; Irabien, A. Carbon dioxide capture from flue gases using a cross-flow membrane contactor and the ionic liquid 1-ethyl-3-methylimidazolium ethylsulfate. *Ind. Eng. Chem. Res.* **2010**, *49*, 11045–11051. [CrossRef]
16. Kuramochi, T.; Ramírez, A.; Turkenburg, W.; Faaij, A. Comparative assessment of CO₂ capture technologies for carbon-intensive industrial processes. *Prog. Energy Combust. Sci.* **2012**, *38*, 87–112. [CrossRef]
17. Luis, P.; van der Bruggen, B. The role of membranes in post-combustion CO₂ capture. *Greenh. Gases* **2013**, *3*, 318–337. [CrossRef]
18. Raganati, F.; Miccio, F.; Ammendola, P. Adsorption of carbon dioxide for post-combustion capture: A review. *Energy Fuels* **2021**, *35*, 12845–12868. [CrossRef]
19. Gonzalez-Olmos, R.; Gutierrez-Ortega, A.; Sempere, J.; Nomen, R. Zeolite versus carbon adsorbents in carbon capture: A comparison from an operational and life cycle perspective. *J. CO₂ Util.* **2022**, *55*, 101791. [CrossRef]
20. Abu-Zahra, M.R.M.; Schneiders, L.H.J.; Niederer, J.P.M.; Feron, H.M.P.; Versteeg, G.F. CO₂ capture from power plants Part I. a parametric study of the technical performance based on monoethanolamine. *Int. J. Greenh. Gas Control* **2007**, *1*, 37–46. [CrossRef]
21. Khaki, E.; Abyar, H.; Nowrouzi, M.; Younesi, H.; Abdollahi, M.; Enderati, M.G. Comparative life cycle assessment of polymeric membranes: Polyacrylonitrile, polyvinylimidazole and poly (acrylonitrile-co-vinylimidazole) applied for CO₂ sequestration. *Environ. Technol. Innov.* **2021**, *22*, 101507. [CrossRef]
22. Wu, F.; Zhou, Z.; Temizel-Sekeryan, S.; Ghamkhar, R.; Hicks, A.L. Assessing the environmental impact and payback of carbon nanotube supported CO₂ capture technologies using LCA methodology. *J. Clean. Prod.* **2020**, *270*, 122465. [CrossRef]
23. Saleh, T.; Yousif, E.; Al-Tikrity, E.; Ahmed, D.; Bufaroosha, M.; Al-Mashhadani, M.; Yaseen, A. Design, synthesis, structure, and gas (CO₂, CH₄, and H₂) storage properties of porous imine-linkage organic compounds. *Mater. Sci. Energy Technol.* **2022**, *5*, 344–352. [CrossRef]
24. Jones, C.W. CO₂ Capture from Dilute Gases as a Component of Modern Global Carbon Management. *Annu. Rev. Chem. Biomol. Eng.* **2011**, *2*, 31–52. [CrossRef] [PubMed]

25. Anselmi, H.; Mirgaux, O.; Bounaceur, R.; Patisson, F. Simulation of post-combustion CO₂ capture, a comparison among absorption, adsorption and membranes. *Chem. Eng. Technol.* **2019**, *42*, 797–804. [\[CrossRef\]](#)
26. Manuilova, A.; Suebsiri, J.; Wilson, M. Should life cycle assessment be part of the environmental impact assessment? Case study: EIA of CO₂ capture and storage in Canada. *Energy Procedia* **2009**, *1*, 4511–4518. [\[CrossRef\]](#)
27. Korre, A.; Nie, Z.; Durucan, S. Life cycle modelling of fossil fuel power generation with post-combustion CO₂ capture. *Int. J. Greenh. Gas Control* **2010**, *4*, 289–300. [\[CrossRef\]](#)
28. Giordano, L.; Roizard, D.; Favre, E. Life cycle assessment of post-combustion CO₂ capture: A comparison between membrane separation and chemical absorption processes. *Int. J. Greenh. Gas Control* **2018**, *68*, 146–163. [\[CrossRef\]](#)
29. Von der Assen, N.; Jung, J.; Bardow, A. Life-cycle assessment of carbon dioxide capture and utilization: Avoiding the pitfalls. *Energy Environ. Sci.* **2013**, *6*, 2721–2734. [\[CrossRef\]](#)
30. Troy, S.; Schreiber, A.; Zapp, P. Life cycle assessment of membrane-based carbon capture and storage. *Clean Technol. Environ. Policy* **2016**, *18*, 1641–1654. [\[CrossRef\]](#)
31. Fayemiwo, K.A.; Chiarasumran, N.; Nabavi, S.A.; Loponov, K.N.; Manovic, V.; Benyahia, B.; Vladislavljevic, G.T. Eco-friendly fabrication of a highly selective amide-based polymer for CO₂ capture. *Ind. Eng. Chem. Res.* **2019**, *58*, 18160–18167. [\[CrossRef\]](#)
32. Khoo, H.H.; Halim, I.; Handoko, A.D. LCA of electrochemical reduction of CO₂ to ethylene. *J. CO₂ Util.* **2020**, *41*, 101229. [\[CrossRef\]](#)
33. Viebahn, P.; Nitsch, J.; Fishedick, M.; Esken, A.; Schüwer, D.; Supersberger, N.; Zuberbühler, U.; Edenhofer, O. Comparison of carbon capture and storage with renewable energy technologies regarding structural, economic, and ecological aspects in Germany. *Int. J. Greenh. Gas Control* **2007**, *1*, 121–133. [\[CrossRef\]](#)
34. Von der Assen, N.; Voll, P.; Peters, M.; Bardow, A. Life cycle assessment of CO₂ capture and utilization: A tutorial review. *Chem. Soc. Rev.* **2014**, *43*, 7982–7994. [\[CrossRef\]](#) [\[PubMed\]](#)
35. Wernet, G.; Bauer, C.; Steubing, B.; Reinhard, J.; Moreno-Ruiz, E.; Weidema, B. The ecoinvent database version 3 (part I): Overview and methodology. *Int. J. Life Cycle Assess.* **2016**, *21*, 1218–1230. [\[CrossRef\]](#)
36. Khoo, H.H.; Tan, R.B. Life cycle investigation of CO₂ recovery and sequestration. *Environ. Sci. Technol.* **2006**, *40*, 4016–4024. [\[CrossRef\]](#) [\[PubMed\]](#)
37. Koorneef, J.; van Keulen, T.; Faaij, A.; Turkenburg, W. Life cycle assessment of a pulverized coal power plant with post-combustion capture, transport and storage of CO₂. *Int. J. Greenh. Gas Control* **2008**, *2*, 448–467. [\[CrossRef\]](#)
38. Odeh, N.A.; Cockerill, T.T. Life cycle GHG assessment of fossil fuel power plants with carbon capture and storage. *Energy Policy* **2008**, *36*, 367–380. [\[CrossRef\]](#)
39. Pehnt, M.; Henkel, J. Life cycle assessment of carbon dioxide capture and storage from lignite power plants. *Int. J. Greenh. Gas Control* **2009**, *3*, 49–66. [\[CrossRef\]](#)
40. Beauchemin, K.A.; Janzen, H.H.; Little, S.M.; McAllister, T.A.; McGinn, S.M. Life cycle assessment of greenhouse gas emissions from beef production in western Canada: A case study. *Agric. Syst.* **2010**, *103*, 371–379. [\[CrossRef\]](#)
41. Nie, Z.; Korre, A.; Durucan, S. Life cycle modelling and comparative assessment of the environmental impacts of oxy-fuel and post-combustion CO₂ capture, transport and injection processes. *Energy Procedia* **2011**, *4*, 2510–2517. [\[CrossRef\]](#)
42. Zapp, P.; Schreiber, A.; Marx, J.; Haines, M.; Hake, J.F.; Gale, J. Overall environmental impacts of CCS technologies-life cycle approach. *Int. J. Greenh. Gas Control* **2012**, *8*, 12–21. [\[CrossRef\]](#)
43. Grant, T.; Anderson, C.; Hooper, B. Comparative life cycle assessment of potassium carbonate and Monoethanolamine solvents for CO₂ capture from post combustion flue gases. *Int. J. Greenh. Gas Control* **2014**, *28*, 35–44. [\[CrossRef\]](#)
44. Zhang, X.; Singh, B.; He, X.; Gundersen, T.; Deng, L.; Zhang, S. Post-combustion carbon capture technologies: Energetic analysis and life cycle assessment. *Int. J. Greenh. Gas Control* **2014**, *27*, 289–298. [\[CrossRef\]](#)
45. Petrescu, L.; Bonalumi, D.; Valenti, G.; Cormos, A.M.; Cormos, C.C. Life Cycle Assessment for supercritical pulverized coal power plants with post-combustion carbon capture and storage. *J. Clean. Prod.* **2017**, *157*, 10–21. [\[CrossRef\]](#)
46. Jens, C.M.; Müller, L.; Leonhard, K.; Bardow, A. To Integrate or Not to Integrate—Techno-Economic and Life Cycle Assessment of CO₂ Capture and Conversion to Methyl Formate Using Methanol, ACS Sustain. *Chem. Eng.* **2019**, *7*, 12270–12280. [\[CrossRef\]](#)
47. Fadeyi, S.; Arafat, H.A.; Abu-Zahra, M.R. Life cycle assessment of natural gas combined cycle integrated with CO₂ post combustion capture using chemical solvent. *Int. J. Greenh. Gas Control* **2013**, *19*, 441–452. [\[CrossRef\]](#)
48. Wang, J.; Yu, Z.; Zeng, X.; Wang, Y.; Li, K.; Deng, S. Water-energy-carbon nexus: A life cycle assessment of post-combustion carbon capture technology from power plant level. *J. Clean. Prod.* **2021**, *312*, 127727. [\[CrossRef\]](#)
49. Mohammed, R.K.; Farzaneh, H. Life Cycle Environmental Impacts Assessment of Post-Combustion Carbon Capture for Natural Gas Combined Cycle Power Plant in Iraq, Considering Grassroots and Retrofit Design. *Energies* **2023**, *16*, 1545. [\[CrossRef\]](#)
50. Olabi, A.G.; Alami, A.H.; Ayoub, M.; Aljaghoub, H.; Alasad, S.; Inayat, A.; Abdelkareem, M.A.; Chae, K.J.; Sayed, E.T. Membrane-based carbon capture: Recent progress, challenges, and their role in achieving the sustainable development goals. *Chemosphere* **2023**, *320*, 137996. [\[CrossRef\]](#)
51. Akan, A.P.; Chau, J.; Sirkar, K.K. Post-combustion CO₂ capture and recovery by pure activated methyl-diethanolamine in crossflow membrane contactors having coated hollow fibers. *Sep. Purif. Technol.* **2020**, *244*, 116427. [\[CrossRef\]](#)
52. DeMontigny, D.; Tontiwachwuthikul, P.; Chakma, A. Using polypropylene and polytetrafluoroethylene membranes in a membrane contactor for CO₂ absorption. *J. Membr. Sci.* **2006**, *277*, 99–107. [\[CrossRef\]](#)

53. Cui, Z.; deMontigny, D. Experimental study of carbon dioxide absorption into aqueous ammonia with a hollow fiber membrane contactor. *J. Membr. Sci.* **2017**, *540*, 297–306. [\[CrossRef\]](#)
54. Mulukutla, T.; Obuskovic, G.; Sirkar, K.K. Novel scrubbing system for post-combustion CO₂ capture and recovery: Experimental studies. *J. Membr. Sci.* **2014**, *471*, 16–26. [\[CrossRef\]](#)
55. Mulukutla, T.; Chau, J.; Obuskovic, G.; Sirkar, K.K. Novel membrane contactor for CO₂ removal from flue gas by temperature swing absorption. *J. Membr. Sci.* **2015**, *493*, 321–328. [\[CrossRef\]](#)
56. ISO14040; Environmental Management—Life Cycle Assessment—Principles and Framework. International Organization for Standardization: Geneva, Switzerland, 2006.
57. ISO14044; Environmental Management—Life Cycle Assessment—Requirements and Guidelines. International Organization for Standardization: Geneva, Switzerland, 2006.
58. Li, G.; Liu, F.; Liu, T.; Yu, Z.; Liu, Z.; Fang, Y. Life cycle assessment of coal direct chemical looping hydrogen generation with Fe₂O₃ oxygen carrier. *J. Clean. Prod.* **2019**, *239*, 118118. [\[CrossRef\]](#)
59. Azapagic, A. Life cycle assessment and its application to process selection, design and optimization. *Chem. Eng. J.* **1999**, *73*, 1–21. [\[CrossRef\]](#)
60. Aldaco, R.; Butnar, I.; Margallo, M.; Laso, J.; Rumayor, M.; Dominguez-Ramos, A.; Irabien, A.; Dodds, P.E. Bringing value to the chemical industry from capture, storage and use of CO₂: A dynamic LCA of formic acid production. *Sci. Total Environ.* **2019**, *663*, 738–753. [\[CrossRef\]](#)
61. Kim, J.; Yang, Y.; Bae, J.; Suh, S. The importance of normalization references in interpreting life cycle assessment results. *J. Ind. Ecol.* **2012**, *17*, 385–395. [\[CrossRef\]](#)
62. Schreiber, A.; Zapp, P.; Kuckshinrichs, W. Environmental assessment of German electricity generation from coal-fired power plants with amine-based carbon capture. *Int. J. Life Cycle Assess.* **2009**, *14*, 547–559. [\[CrossRef\]](#)
63. Goodarzi, A.A.; Anikin, A.; Pearson, D.D. Environmental sources of ionizing radiation and their health consequences. In *Genome Stability from Virus to Human Application*; Kovalchuk, I., Kovalchuk, O., Eds.; Academic Press: Cambridge, MA, USA; Elsevier: Amsterdam, The Netherlands, 2016; pp. 569–581.
64. Jones, J.A.; Casey, R.C.; Karovia, F. Ionizing radiation as a carcinogen. In *Comprehensive Toxicology*, 2nd ed.; Elsevier: Amsterdam, The Netherlands, 2010; Volume 14, pp. 181–228. [\[CrossRef\]](#)
65. Ortiz-Reyes, E.; Anex, R.P. A life cycle impact assessment method for freshwater eutrophication due to the transport of phosphorous from agricultural production. *J. Clean. Prod.* **2018**, *177*, 474–482. [\[CrossRef\]](#)
66. Xia, R.; Zhang, Y.; Critto, A.; Wu, J.; Fan, J.; Zheng, Z.; Zhang, Y. The potential impacts of climate change factors on freshwater eutrophication: Implications for research and countermeasures of water management in China. *Sustainability* **2016**, *8*, 229. [\[CrossRef\]](#)
67. Ho, K.C.; Teoh, Y.X.; Teow, Y.H.; Mohammad, A.W. Life cycle assessment (LCA) of electrically-enhanced POME filtration: Environmental impacts of conductive-membrane formulation and process operating parameters. *J. Environ. Manag.* **2021**, *277*, 111434. [\[CrossRef\]](#)
68. Borrión, A.L.; Khraisheh, M.; Benyahia, F. Environmental life cycle impact assessment of Gas-to Liquid processes. In Proceedings of the 3rd International Gas Processing Symposium, Doha, Qatar, 5–7 March 2012.
69. Fairbrother, A.; Hope, B. Terrestrial Toxicology. In *Encyclopedia of Toxicology*; Wexler, P., Ed.; Elsevier: Limerick, Ireland, 2005; pp. 138–142.
70. Chakraborty, S.; Tiedemann, A.V.; Teng, P.S. Climate change: Potential impact on plant diseases. *Environ. Pollut.* **2000**, *108*, 317–326. [\[CrossRef\]](#)
71. Hobbie, S.E.; Grimm, N.B. Nature-based approaches to managing climate change impacts in cities. *Philos. Trans. R. Soc. B* **2020**, *375*, 20190124. [\[CrossRef\]](#)
72. Guinée, J.; Heijungs, R. A proposal for the classification of toxic substances within the framework of life cycle assessment of products. *Chemosphere* **1993**, *26*, 1925–1944. [\[CrossRef\]](#)
73. Hertwich, E.G.; Mateles, S.F.; Pease, W.S.; McKone, T.E. Human toxicity potentials for life-cycle assessment and toxics release inventory risk screening. *Environ. Toxicol. Chem.* **2001**, *20*, 928–939. [\[CrossRef\]](#)
74. Irvine, I.C.; Greaver, T.; Phelan, J.; Sabo, R.D.; Van Houtven, G. Terrestrial acidification and ecosystems services: Effects of acid rain on bunnies, baseball, and Christmass trees. *Ecosphere* **2017**, *8*, e01857. [\[CrossRef\]](#)
75. Pardo, L.H.; Fenn, M.E.; Goodale, C.L.; Geiser, L.H.; Driscoll, C.T.; Allen, E.B.; Baron, J.S.; Bobbink, R.; Bowman, W.D.; Clark, C.M.; et al. Effects of nitrogen deposition and empirical nitrogen critical loads for ecoregions of the United States. *Ecol. Appl.* **2011**, *21*, 3049–3082. [\[CrossRef\]](#)
76. Roy, P.O.; Azevedo, L.B.; Margni, M.; van Zelm, R.; Deschênes, L.; Huijbregts, M.A.J. Characterization factors for terrestrial acidification at the global scale: A systematic analysis of spatial variability and uncertainty. *Sci. Total Environ.* **2014**, *500–501*, 270–276. [\[CrossRef\]](#)
77. Bolaji, B.O.; Huan, Z. Ozone depletion and global warming: Case for the use of natural refrigerant—A review. *Renew. Sustain. Energy Rev.* **2013**, *18*, 49–54. [\[CrossRef\]](#)
78. Karasu, H.; Dincer, I. Life cycle assessment of integrated thermal energy storage systems in buildings: A case study in Canada. *Energy Build.* **2020**, *217*, 109940. [\[CrossRef\]](#)

79. Hayashi, K.; Nakagawa, A.; Itsubo, N.; Inaba, A. Expanded damage function of stratospheric ozone depletion to cover major endpoints regarding life cycle impact assessment. *Int. J. LCA* **2006**, *11*, 150–161. [[CrossRef](#)]
80. Zhang, J.; Wuebbles, D.; Kinnison, D.E.; Saiz-Lopez, A. Revising the ozone depletion potentials metric for short-lived chemicals such as CF₃I and CH₃I. *J. Geophys. Res. Atmos.* **2020**, *125*, e2020JD032414.
81. Tong, H.; Zhang, Y.; Filippi, A.; Wang, T.; Li, C.; Liu, F.; Leppla, D.; Kourtchev, I.; Wang, K.; Keskinen, H.M.; et al. Radical formation by fine particulate matter associated with highly oxygenated molecules. *Environ. Sci. Technol.* **2019**, *53*, 12506–12518. [[CrossRef](#)] [[PubMed](#)]
82. Zheng, M.; Yan, C.; Zhu, T. Understanding sources of fine particulate matter in China. *Philos. Trans. R. Soc. A* **2020**, *378*, 20190325. [[CrossRef](#)]
83. Zhou, H.; Zhao, h.; Hu, J.; Li, M.; Feng, Q.; Qi, J.; Zongbo, S.; Mao, H.; Jin, T. Primary particulate matter emissions and estimates of secondary organic aerosol formation potential from the exhaust of a China V diesel engine. *Atmos. Environ.* **2019**, *218*, 116987. [[CrossRef](#)]
84. Jackson, M.; Eadsforth, C.; Schowanek, D.; Delfosse, T.; Riddle, A.; Budgen, N. Comprehensive review of several surfactants in marine environments: Fate and ecotoxicity. *Environ. Toxicol. Chem.* **2016**, *35*, 1077–1086. [[CrossRef](#)]
85. Aurisano, N.; Albizzati, P.F.; Hauschild, M.; Fantke, P. Extrapolation factors for characterizing freshwater ecotoxicity effects. *Environ. Toxicol. Chem.* **2019**, *38*, 2568–2582. [[CrossRef](#)]
86. Papasavva, S.; Beltramo, M.A. An index of the ecological impacts of water toxics emitted to freshwater ecosystems. *Hum. Ecol. Risk Assess.* **2006**, *12*, 476–492. [[CrossRef](#)]
87. Meyer-Reil, L.A.; Köster, M. Eutrophication of Marine Waters: Effects on Benthic Microbial Communities. *Mar. Pollut. Bull.* **2000**, *41*, 255–263. [[CrossRef](#)]
88. Zhang, W.; Li, J.; Chen, G.; You, W.; Jiang, Y.; Sun, W. Experimental Study of Mass Transfer in Membrane Absorption Process Using Membranes with Different Porosities. *Ind. Eng. Chem. Res.* **2010**, *49*, 6641. [[CrossRef](#)]

Disclaimer/Publisher's Note: The statements, opinions and data contained in all publications are solely those of the individual author(s) and contributor(s) and not of MDPI and/or the editor(s). MDPI and/or the editor(s) disclaim responsibility for any injury to people or property resulting from any ideas, methods, instructions or products referred to in the content.